Line parameters of acetylene in the 1.9 and 1.7-μm spectral regions

Oleg M. Lyulin, David Jacquemart, Nelly Lacome, Valery I. Perevalov, Jean-Yves Mandin

▶ **To cite this version:**

Oleg M. Lyulin, David Jacquemart, Nelly Lacome, Valery I. Perevalov, Jean-Yves Mandin. Line parameters of acetylene in the 1.9 and 1.7-μm spectral regions. Journal of Quantitative Spectroscopy and Radiative Transfer, 2008, 109 (10), pp.1856-1874. 10.1016/j.jqsrt.2007.11.016 . hal-00745582

HAL Id: hal-00745582

https://hal.sorbonne-universite.fr/hal-00745582v1

Submitted on 25 Oct 2012

HAL is a multi-disciplinary open access archive for the deposit and dissemination of scientific research documents, whether they are published or not. The documents may come from teaching and research institutions in France or abroad, or from public or private research centers.

L'archive ouverte pluridisciplinaire **HAL**, est destinée au dépôt et à la diffusion de documents scientifiques de niveau recherche, publiés ou non, émanant des établissements d'enseignement et de recherche français ou étrangers, des laboratoires publics ou privés.

Line parameters of acetylene in the 1.9 and 1.7-μm spectral regions

O.M. Lyulin[1], D. Jacquemart[2*], N. Lacome[2], V.I. Perevalov[1], J.-Y. Mandin [3]

[1] *Laboratory of Theoretical Spectroscopy, Institute of Atmospheric Optics, Siberian Branch, Russian Academy of Sciences, 1, Akademicheskii av.,634055 Tomsk, Russia*

[2] *Université Pierre-et-Marie-Curie-Paris 6, Laboratoire de Dynamique, Interactions et Réactivité, CNRS, UMR 7075, Case courrier 49, Bât F 74, 4, place Jussieu, 75252 Paris Cedex 05, France*

[3] *Laboratoire de Physique Moléculaire pour l'Atmosphère et l'Astrophysique,Université Pierre et Marie Curie-Paris 6; CNRS, UMR 7092, Case courrier 76,4, place Jussieu, 75252 Paris Cedex 05, France*

Received 2007

[*] Corresponding author. Tel.: + 33-1-44-27-36-82; fax: + 33-1-44-27-30-21.
E-mail address: jacquemart@spmol.jussieu.fr.

Abstract

Using FT spectra (Bruker IFS 120, unapodized resolution ≈ 0.01 cm^{-1}) of acetylene $^{12}C_2H_2$, line positions and intensities, as well as self-broadening and shifting coefficients are measured for about 550 lines of 13 bands between 5000 and 6000 cm^{-1}. A multispectrum fitting procedure is used to retrieve line parameters from 4 experimental spectra recorded at different pressures. An absolute wavenumber calibration has been performed using isolated acetylene line positions around 5900 cm^{-1}. The average accuracy of the line parameters obtained in this work is estimated to be $\pm$ 0.001 cm^{-1} for line positions, 5-10% for line intensities depending on the transitions, about 5% for self-broadening coefficients, and $\pm$ 0.005 $cm^{-1}.atm^{-1}$ for self-shifting coefficients. For each studied band, the vibrational transition dipole moment squared and the empirical Herman-Wallis coefficients are adjusted. The measured line intensities allow to obtain the effective dipole moment parameters of the global approach for the ΔP = 8 and 9 series. A polynomial description of the rotational dependence of self-broadening coefficients is performed. A weak rotational dependence of the self-shifting coefficients is observed.

Key words: Acetylene; Infrared; Vibration-rotation transitions; Fourier transform spectroscopy; Line intensities; Broadening coefficients; Shifting coefficients

1. Introduction

The present paper is devoted to an extension of the previous measurements of the line intensities of acetylene [1-12] in order to elaborate a complete database for this molecule. In the 1.9-μm spectral region, the only work published to our knowledge is the one by Smith and Winn [13], in which spectroscopic constants and relative band intensities of four cold bands, namely the $\nu_2+(4\nu_4+\nu_5)^1\mathrm{II}$, $\nu_3+3\nu_4^1$, $\nu_2+\nu_3$ and $2\nu_2+(\nu_4+\nu_5)^0_+$ bands have been presented. In the 1.7-μm spectral region, the positions of eight bands have been published by Keppler et al. [14].

In the present work, about 550 transitions of 13 bands, namely the $\nu_2+(4\nu_4+\nu_5)^1\mathrm{II}$, $\nu_3+3\nu_4^1$, $\nu_1+(2\nu_4+\nu_5)^1\mathrm{I}$, $\nu_2+(2\nu_4+3\nu_5)^1\mathrm{III}$, $\nu_1+3\nu_5^1$, $\nu_2+\nu_3$, $2\nu_2+(\nu_4+\nu_5)^0_+$, $\nu_2+\nu_3+\nu_4^1$, $2\nu_2+(2\nu_4+\nu_5)^1\mathrm{II}$, $\nu_1+\nu_3-\nu_4^1$, $2\nu_3-\nu_5^1$, $\nu_1+\nu_2+2\nu_4^0-\nu_5^1$ and $2\nu_1-\nu_5^1$ bands, have been studied between 5000 and 6000 cm^{-1}. The line positions, intensities, self-broadening and self-shifting coefficients have been measured using a multispectrum fitting procedure [15] applied to four experimental spectra recorded for different pressures of C_2H_2. For each studied band, the vibrational transition dipole moment squared and empirical Herman-Wallis coefficients have been obtained. The global effective operator approach has also been applied to model the measured line intensities. The 13 effective dipole moment parameters describing the line intensities of the ΔP = 8 series (transitions around 1.9 μm) and 11 effective dipole moment parameters of the ΔP = 9 series (transitions around 1.7 μm) have been retrieved. An empirical polynomial expansion has been used to model the observed rotational dependence of the self-broadening coefficients.

The experimental procedure and the methodology of the analysis are presented in Sections 2 and 3 respectively. Section 4 is devoted to the analysis and the modelling of the spectral line parameters.

2. Experimental procedure

To record the spectra, the rapid scan Bruker IFS 120 HR interferometer of the LADIR (Paris) was used. The unapodized spectral resolution used for each spectrum was equal to 10^{-2} cm^{-1} ($0.9/\Delta_{max}$) that corresponds to a maximal optical path difference of 90 cm. The interferometer was equipped with a CaF_2 beam splitter, an InSb detector, a Globar source, and an optical filter covering the 4800 - 6400 cm^{-1} spectral region. The bandpath of the filter has

been chosen quite wide allowing the simultaneous recording of two different regions of the acetylene spectrum: around 1.9 μm and 1.7 μm. The lines of both spectral regions have been analyzed in the present work. Four spectra have been recorded with various C_2H_2 pressures; experimental conditions are summarized in Table 1. The whole optical path was under vacuum and a multipass cell of one meter base length was used for a total absorption path of 1615 ± 1 cm. The cell was equipped with KCl windows. The commercial gas sample, furnished by Air Liquide Alphagaz, with a stated purity of 99.70 % in natural abundances, was used without further purification. The temperature of the gas in the cell was recorded via four platinum probes at different places in the cell. The accuracy on the temperature measurements has been estimated to be ± 1 K. The accuracy takes into account small temperature gradients inside the cell. The pressure of the gas was measured with a capacitive MKS Baratron manometer with an accuracy estimated to be equal to ± 1%. Every scan among the 300 recorded for every spectrum has then been individually transformed to spectrum using the Fourier transform procedure included in the Bruker software OPUS package [16], selecting a Mertz phase error correction [17, 18].

3. Line parameter measurements

3.1. The multispectrum fitting procedure

Line parameters have been retrieved using a multispectrum procedure [15] that adjusts a calculated spectrum to each laboratory spectrum simultaneously. In this way, line positions, line intensities, self- broadening and –shifting coefficients have been directly retrieved from the simultaneous fit of four experimental spectra.

At 296 K and 5500 cm^{-1}, the Doppler half-width at half-maximum (HWHM) is equal to 0.005 cm^{-1} for $^{12}C_2H_2$. The half-width at half-maximum of the apparatus function is mainly due to the limitation of the optical path difference and is equal to 0.003 cm^{-1}. Since the values of broadening coefficients are about 0.15 $cm^{-1}atm^{-1}$ [3,19], the collisional half-width at half-maximum (equal to the product: self-broadening coefficient × partial pressure of $^{12}C_2H_2$) is between 0.005 and 0.025 cm^{-1} depending on the experimental spectrum. Therefore the collisional width can be determined from the spectra at higher pressures. A linear pressure dependence of the line positions has also been observed, allowing the measurement of self-shifting coefficients. As a consequence, the line position at zero pressure, the line intensity,

and the self-broadening and self-shifting coefficients of a same transition are adjusted simultaneously to the 4 spectra. A Voigt profile has been used, without detecting any signatures that would result from collisional narrowing effect [20]. The line intensities obtained by using the multispectrum procedure are for temperature 296 K and for pure $^{12}C_2H_2$. Since the spectra are recorded at temperatures slightly different from 296 K, a temperature conversion of the line intensities has been done using the total partition function of Ref. [21]. The weak temperature effect on the broadening and shifting coefficients has been neglected because the temperatures were very close to 296 K.

3.2. Preliminaries

3.2.1. Apparatus function and numerical treatment of the spectra

The spectra were not numerically apodized. They were over sampled (oversampling ratio: 8) by post-zero filling the interferograms, but no additional interpolation was performed.

For each spectrum, the apparatus function was calculated [1] performing numerically the Fourier transform of the optical weighting function of the interferogram, due to the throughput, truncated at the maximum optical path difference. To avoid distortion effects, an apparatus function was calculated for each studied transition, in order to take into account the wavenumber dependence of the optical weighting [1].

In the definition of the apparatus function, the aperture and the focal length of the collimator are sensitive parameters. The nominal value of the focal length (418 mm) was used but the value of the aperture has been fitted for several isolated transitions. Finally an effective radius value of the aperture of 1.2 ± 0.1 mm has been obtained, differing from its nominal value of 1mm. Such a difference has already been obtained in previous works [3,22] and can be imputed to a slightly divergence of the beam.

Furthermore, a weak multiplicative channeling spectrum, due to the cell windows and to the optical filter, was observed. The effect of these multiplicative channeling spectra are negligible for the determination of the continuous background, since the adjusted spectral domains used are always less than the half-period of the channel spectra (see Ref. [15])).

3.2.2. Wavenumbers calibration

The wavenumber scale has been calibrated using the positions of $^{12}C_2H_2$ transitions between 5700 and 6000 cm^{-1}. The absolute wavenumbers from the work of Keppler et al. [14] were taken as standard. The quantity $\varepsilon = (\nu_{[Keppler]} - \nu_{this\ work}) / \nu_{[Keppler]}$ has been calculated for 38 isolated transitions of several bands of $^{12}C_2H_2$. Averaging the ε quantity for all 38 transitions, the mean value $<\varepsilon> = 2.9\times10^{-6}$ has been found with 1 SD = 0.1×10^{-6}. This corresponds to a wavenumber deviation of 15.1×10^{-3} cm^{-1} at 5200 cm^{-1} with 1 SD = 0.5×10^{-3} cm^{-1}. Considering the dispersion of the wavenumber calibration, and the accuracy of the line position measurements given by Keppler et al. [14], the accuracy of the wavenumber calibration has been estimated to be equal to 0.5×10^{-3} cm^{-1}.

3.2.3. Assignment of three new bands of $^{12}C_2H_2$ in the region 1.9 μm

Because more bands have been observed in this work than in Ref. [13], the global effective vibration-rotation Hamiltonian [23] has been used to make a prediction. This prediction has allowed to assign many transitions belonging to 7 cold bands of acetylene in this region: the $\nu_2 + (4\nu_4 + \nu_5)^1\mathrm{II}$, $\nu_3 + 3\nu_4^1$, $\nu_1 + (2\nu_4 + \nu_5)^1\mathrm{I}$, $\nu_2 + (2\nu_4 + 3\nu_5)^1\mathrm{III}$, $\nu_1 + 3\nu_5^1$, $\nu_2 + \nu_3$ and $2\nu_2 + (\nu_4 + \nu_5)_+^0$ bands. Many of these transitions were never assigned. We also observed the $\nu_3 + (\nu_4 + 2\nu_5)^1\mathrm{II}$ band, but it was too weak to measure line parameters with an acceptable accuracy.

4. Results

Line parameters of about 550 transitions belonging to 13 bands have been deduced between 5000 and 6000 cm^{-1} using a multispectrum fitting procedure [15]. Because of the experimental conditions, the lines of two bands published by Keppler et al. [14] were not strong enough in our spectra to allow the measurement of their line parameters. Note that the $\nu_2 + \nu_3$ and $2\nu_2 + (\nu_4 + \nu_5)_+^0$ bands are parallel bands, whereas the other bands are perpendicular ones with strong *Q* branches. The accuracy of the measured line parameters have been estimated to be about 10^{-3} cm^{-1} for positions, 5-10% for line intensities depending on the intensity of the line, 5% for self-broadening coefficients, and ± 0.005 $cm^{-1}.atm^{-1}$ for self-shifting coefficients. In Tables 2-5 are presented the sets of the measured line parameters of four bands taken as examples. The complete set of line parameters measured in this work is

available as Supplementary materials. The obtained results and their theoretical reductions are detailed in the following sub-sections

4.1. Line positions

Before performing the measurements, the line positions of C_2H_2 in the 1.7- and 1.9-μm spectral regions have been predicted using the vibration-rotation effective Hamiltonian operator [23] in which the greater part of resonances are taken into account. The measurement of the line positions at zero pressure, together with the self-pressure shift coefficient has been done using the multispectrum fitting procedure which was applied to the four experimental spectra beforehand calibrated (see Section 3.2.2). Taking into account the accuracy of the wavenumber calibration, as well as the precision of the determination of the centers of the broadened lines, the global accuracy of the line positions at zero pressure is estimated to be about 10^{-3} cm^{-1}. These experimental line positions and those measured in Refs. [7-9] will be used to improve the set of the global effective Hamiltonian parameters for the acetylene molecule.

4.2. Line intensities

Based on the experimental conditions, the accuracy of the measured line intensities has been estimated to be about 5% for the strongest transitions and 10% for the weakest ones. Two different analyses of the measured line intensities have been applied. First, a theoretical global treatment [24] has been used to obtain the effective dipole moment parameters for the $\Delta P = 8$ and $\Delta P = 9$ series of transitions. Then, a semi-empirical treatment has been performed with the usual Herman-Wallis coefficients.

4.2.1. Effective dipole moment

In a general form, the intensity $S_{V'J'\varepsilon'\leftarrow VJ\varepsilon}$ (expressed in $cm^{-1}/(molecule \cdot cm^{-2})$ at temperature T in K) of an absorption line corresponding to the transition $V'J'\varepsilon' \leftarrow VJ\varepsilon$ (where V and J are respectively the vibrational index and the angular momentum quantum number, and where $\varepsilon = \pm 1$ is the parity) is related to the vibration-rotation transition moment squared $W_{V'J'\varepsilon'\leftarrow VJ\varepsilon}$ by the well known equation:

$$S_{V'J'\varepsilon'\leftarrow VJ\varepsilon}(T)=\frac{8\pi^3}{3hc}Cg_{VJ\varepsilon}\frac{\nu_{V'J'\varepsilon'\leftarrow VJ\varepsilon}}{Q(T)}\exp\left(-\frac{hcE_{VJ\varepsilon}}{kT}\right)\left[1-\exp\left(-\frac{hc\nu_{V'J'\varepsilon'\leftarrow VJ\varepsilon}}{kT}\right)\right]W_{V'J'\varepsilon'\leftarrow VJ\varepsilon} \quad (1)$$

where $E_{VJ\varepsilon}$ is the energy of the lower state, $\nu_{V'J'\varepsilon'\leftarrow VJ\varepsilon}$ is the wavenumber of the transition, $Q(T)$ is the total internal partition function at temperature T, C is the isotopic abundance, and $g_{VJ\varepsilon}$ is the nuclear statistical weight. In this work, the partition function $Q(T)$ is taken from Gamache et al. [21], and the value of isotopic abundance is $C = 1$ because we used the measured line intensities recalculated for pure $^{12}C_2H_2$.

Within the framework of the method of effective operators, the vibration-rotation transition moment squared could be calculated using the eigenfunctions of the global effective Hamiltonian. We have used the eigenfunctions of the effective Hamiltonian [23] parameters of which are fitted to the measured line positions between 60 and 10000 cm^{-1}. This Hamiltonian is based on the assumption of Abbouti Temsamani and Herman [25] that the vibrational energy levels of acetylene molecule have a cluster structure due to the following approximate relations between harmonic frequencies:

$$\omega_1 \approx \omega_3 \approx 5\omega_4 \approx 5\omega_5, \quad (2)$$

$$\omega_2 \approx 3\omega_4 \approx 3\omega_5. \quad (3)$$

A cluster (polyad) of vibrational states is then defined by the integer value P (pseudo-quantum number) that is equal to:

$$P = 5V_1 + 3V_2 + 5V_3 + V_4 + V_5. \quad (4)$$

The operators of resonance interactions (interactions between vibration-rotation states belonging to the same polyad) are included into the expression of the effective Hamiltonian, and those of nonresonance interactions (interactions between vibrational states belonging to different polyads) are accounted for by effective Hamiltonian parameters [23].

The vibration-rotational states of a linear molecule in its ground electronic state, within the framework of the effective operator approach, can be labeled by four numbers: P, N, J, ε, where N is the ranking index of the eigenvalues in a (P, ε, J) block. The eigenfunctions of effective Hamiltonian can be presented in the following form:

$$\Psi_{PNJ\varepsilon}^{eff} = \sum_{\substack{5V_1+3V_2+5V_3+V_4+V_5=P \\ \ell_4\ \ell_5}}{}^{J} C_{PN\varepsilon}^{V_1V_2V_3V_4V_5\ell_4\ell_5}\left|V_1V_2V_3V_4V_5\ell_4\ell_5\,J\,K\,\varepsilon\right\rangle, \quad (5)$$

where $\left|V_1 V_2 V_3 V_4 V_5 \ell_4 \ell_5 J K \varepsilon\right\rangle$ is the Wang-type basis function (see Ref. [24]), ${}^{J}C_{PN\varepsilon}^{V_1V_2V_3V_4V_5\ell_4\ell_5}$ is the expansion coefficient; K is the quantum number of the projection of the angular momentum on the z axis of the molecular-fixed frame ($K = |\ell_4 + \ell_5|$ for $^{12}C_2H_2$).

The upper levels of the studied transitions in the region 1.9-μm transitions belong to eighth polyad of acetylene ($P = 8$). The scheme of the interactions of the vibrational levels in this polyad is quite complicated and sometimes the transition assignment in terms of harmonic oscillator quantum numbers is not completely unambiguous. As an example, the most important contributions of the basis wavefunctions to the studied states belonging to the ($P = 8$, $\varepsilon = 1$, $J = 3$) block are given in Table 6. Contrary to the 1.9-μm region the most of upper levels of the transitions studied in the region 1.7-μm are well isolated except the two interacting states $2\nu_3$ and $\nu_1 + \nu_2 + 2\nu_4{}^0$.

Using eigenfunctions (5) the vibration-rotation transition moment squared can be written [24] in the following way:

$$W_{P'N'J'\varepsilon'\leftarrow PNJ\varepsilon} = (2J+1)\left| \sum_{\substack{5V_1+3V_2+5V_3+V_4+V_5=P \\ \ell_4 \square_5}} \sum_{\substack{5\Delta V_1+3\Delta V_2+5\Delta V_3+\Delta V_4+\Delta V_5=\Delta P \\ \Delta\ell_4\ \Delta\ell_5}} {}^{J}C_{PN\varepsilon}^{V_1\ V_2\ V_3 V_4 V_5 \ell_4 \ell_5} \right.$$

$$\times {}^{J'}C_{P'N'\varepsilon'}^{V_1+\Delta V_1\, V_2+\Delta V_2\, V_3+\Delta V_3\, V_4+\Delta V_4\, V_5+\Delta V_5\, \ell_4+\Delta\ell_4\, \ell_5+\Delta\ell_5} \quad M_{\Delta V}^{\Delta\ell_4\,\Delta\ell_5}\, \Phi_{\Delta J\ \Delta K}(\mathrm{J},\mathrm{K})$$

$$\times \sqrt{f_{\Delta V}^{\Delta\ell_4\,\Delta\ell_5}(V,\ell_4,\ell_5)\left(1+\delta_{\ell_4,0}\,\delta_{\ell_5,0}+\delta_{\ell_4+\Delta\ell_4,0}\,\delta_{\ell_5+\Delta\ell_5,0}-2\delta_{\ell_4,0}\,\delta_{\ell_5,0}\delta_{\ell_4+\Delta\ell_4,0}\,\delta_{\ell_5+\Delta\ell_5,0}\right)}$$

$$\left. \times\left(1+\sum_i \kappa_i^{\Delta V\ \Delta\ell_4\,\Delta\ell_5} V_i + {}^{\Delta V}F_{\Delta J\ \Delta K}^{\Delta\ell_4\,\Delta\ell_5}(J,K)\right)\right|^2, \qquad (6)$$

where the functions $\Phi_{\Delta J\ \Delta K}(J,K)$ for $\Delta K = 0,\pm 1$ are the Clebsch-Gordon coefficients:

$$\Phi_{\Delta J\ \Delta K}(J,K) = \left(1\Delta K\ \ JK \middle| J+\Delta J\ K+\Delta K\right). \qquad (7)$$

The functions $f_{\Delta V}^{\Delta\ell_4\,\Delta\ell_5}(V,\ell_4,\ell_5)$ and the Herman-Wallis type function ${}^{\Delta V}F_{\Delta J\ \Delta K}^{\Delta\ell_4\,\Delta\ell_5}(J,K)$ are given in Ref. [24]. Note that Eq. (6) is equivalent to Eq. (12) of Ref. [24] in the case of the bands observed in this work.

The parameters of the matrix elements of the effective dipole moment operator are:

$$M_{\Delta V}^{\Delta\ell_4\,\Delta\ell_5} = M_{\Delta V}^{-\Delta\ell_4\,-\Delta\ell_5},\ \kappa_i^{\Delta V\,\Delta\ell_4\,\Delta\ell_5} = \kappa_i^{\Delta V\,-\Delta\ell_4\,-\Delta\ell_5}\,(i = 1,2,3,4,5), \qquad (8)$$

$$b_J^{\Delta V\,\Delta\ell_4\,\Delta\ell_5} = b_J^{\Delta V\,-\Delta\ell_4\,-\Delta\ell_5},\ d_{JQ}^{\Delta V\,\Delta\ell_4\,\Delta\ell_5} = d_{JQ}^{\Delta V\,-\Delta\ell_4\,-\Delta\ell_5}.$$

These parameters, involved in Eq. (6), describe simultaneously the line intensities of hot and cold bands belonging to the same ΔP series.

In the 1.9-μm spectral region (ΔP=8), the fit of 325 measured line intensities belonging to seven cold bands has led to the determination of 13 effective dipole moment parameters that are presented in the upper part of Table 7. This set of parameters contains seven vibrational parameters (each band has its own vibrational parameter) and 6 rotational parameters. The line intensities calculated with the effective dipole moment parameters of the Table 7 are presented in the fourth column of the Tables 2-3. The bands statistics is presented in the upper part of the Table 8. All observed intensities have been weighted in the fit by the 7% uncertainty and the value of standard deviation χ=0.87 has been obtained. It should be emphasized that the fit could be performed without parameters $M_{00130}^{10}, d_{JQ}^{0013010}$. The latter gives the standard deviation χ=0.97. But in this case the residuals for the *Q* branch of the $\nu_3 + 3\nu_4{}^1$ band have a definite rotational dependence.

In the 1.7-μm spectral region (ΔP=9), the 11 effective dipole moment parameters have been obtained in the result of the fit of 220 measured line intensities of 6 bands (second part of the Table 7). Similarly to the previous region this set of parameters contains one vibrational parameter for each band and 5 rotational parameters. The line intensities calculated with the effective dipole moment parameters of Table 7 are presented in the fourth column of the Tables 4-5. The bands statistics is presented in the second part of the Table 8. All observed intensities have been weighted in the fit by the 7% uncertainty and the value of standard deviation χ=0.58 has been obtained.

4.2.2. Vibrational transition dipole moment squared, and Herman-Wallis factor

In this section we present the empirical treatment of the measured line intensities. For each band, the vibrational transition dipole moment squared and the Herman-Wallis coefficients have been calculated. Using this empirical approach, the vibration-rotation transition moment squared can be expressed as the product of the transition dipole moment squared and the Hönl-London factor:

$$W_{V'J'\varepsilon'\leftarrow VJ\varepsilon} = \frac{1}{g_l}\left|R\right|^2 L(J,K), \tag{9}$$

where g_l is a weight introduced in the case of the bands with ℓ-type doubling (g_l is equal to 2 when K is greater than 0 for both upper and lower vibrational levels; otherwise, g_l is equal to 1); $\left|R\right|^2$ is transition dipole moment squared; $L(J,K)$ is the Hönl-London factor. For perpendicular bands ($\Delta K = \pm 1$) of linear molecules, the Hönl-London factors are given [26] by:

$$L(J,K) = (J+2+K\cdot\Delta K)(J+1+K\cdot\Delta K)/[2(J+1)] \text{ (}R\text{-branch)}, \tag{10}$$

$$L(J,K) = (J+1+K\cdot\Delta K)(J-K\cdot\Delta K)(2J+1)/[2J(J+1)] \text{ (}Q\text{-branch)}, \tag{11}$$

$$L(J,K) = (J-1-K\cdot\Delta K)(J-K\cdot\Delta K)/[2J] \text{ (}P\text{-branch)}. \tag{12}$$

For parallel bands ($\Delta K = 0$), the Hönl-London factors are given [26] by:

$$L(J,K) = (J+1+K)(J+1-K)/(J+1) \quad (R\text{-branch}), \tag{13}$$

$$L(J,K) = (2J+1)K^2/[J(J+1)] \quad (Q\text{-branch}), \tag{14}$$

$$L(J,K) = (J+K)(J-K)/J \quad (P\text{-branch}). \tag{15}$$

The transition dipole moment squared $\left|R\right|^2_{obs}$, calculated from the measured line intensities using Eqs. (1,9), are presented in Tables 2-5. For linear molecule as acetylene, the rotational dependence of the transition dipole moment squared can be expressed by the well known expansion:

$$\left|R\right|^2 = \left|R_0\right|^2 F(m), \tag{16}$$

where $|R_0|^2$ is the vibrational transition dipole moment squared, and $F(m)$ is the empirical Herman-Wallis factor (m being equal to $-J$ for the P branch, J for the Q branch, and $J+1$ for the R branch) which can be expressed as following:

for P and R branches: $$F^{RP}(m) = (1 + A_1^{RP} m + A_2^{RP} m^2)^2, \tag{17}$$

for Q branches: $$F^{Q}(m) = \left[1 + A_2^{Q} m^2\right]^2, \tag{18}$$

where A_1^{RP}, A_2^{RP}, and A_2^{Q} are the Herman-Wallis coefficients.

For each band, the vibrational transition dipole moment squared and the Herman-Wallis coefficients have been obtained using Eqs. (16-18). These coefficients are given in Table 9. Using them the transition dipole moments squared $|R|^2_{calc}$ have been calculated and are presented in Tables 2-5, as well as their differences with $|R|^2_{obs}$. The experimental and calculated values of the transition dipole moments squared $|R|^2_{obs}$ and $|R|^2_{calc}$ have been plotted versus the rotational quantum number *m* for three bands, and are presented in Figs. 1-3.

The effective dipole moment approach (see Section 4.2.1) and the semi-empirical approach involving the Herman-Wallis coefficients have both led to a good agreement between the measurements and the calculation. The average discrepancy between the $|R|^2_{obs}$ and $|R|^2_{calc}$ values is equal to (0.2 ± 4.4) % in the case of empirical approach. Concerning the results obtained with the effective dipole moment, the average discrepancy between the observed and calculated line intensities is equal to (0.3 ± 5.3) %. The two models give similar results, but it is worth noticing that the effective dipole moment model is supposed to give better extrapolations.

4.3. Self-broadening coefficients

The self-broadening coefficients obtained with the multispectrum fitting procedure are presented in Tables 2-5, and have been plotted for each band versus rotational quantum number *m*, showing no significant vibrational dependence. As an example, the rotational dependence of the broadening coefficients is presented in Figs. 4 and 5 respectively for one parallel and one perpendicular band in the 1.9-µm spectral region. Very close values and same behavior versus rotational quantum number can be seen in these figures for the self-broadening coefficients of these two bands. In Figs. 6 and 7, all measured self-broadening coefficients have been gathered respectively for the 1.9- and 1.7-µm spectral regions. These figures show the same rotational dependence for self-broadening coefficient of different bands in these regions. These results together with those earlier published [3,19,27] allow us to confirm the fact that the vibrational dependence of self-broadening coefficients of acetylene can be neglected at nowadays accuracy level of their determination. The rotational dependence of the self-broadening coefficients has been modeled using an empirical forth- and fifth-order polynomial expansion:

$$\gamma^{0}_{self} = A_0 + B_1 |m| + B_2 |m|^2 + B_3 |m|^3 + B_4 |m|^4 + B_5 |m|^5. \quad (19)$$

The expansion coefficients obtained for the 1.9- and 1.7-μm spectral regions are given in Table 10. The self-broadening coefficients calculated using Eq. (19) are also plotted in Figs. 6 and 7 together with the observed values. As one can see from these figures there is good agreement between observed and calculated values in both spectral regions. The self-broadening coefficients calculated with polynomial expansion given in reference [3] are also presented in the Fig. 6 as empty triangles. Finally, all self-broadening coefficients obtained in both spectral regions were simultaneously fitted using Eq. (19). The respective expansion coefficients are given in the last row of Table 10.

The average discrepancy between the calculated self-broadening coefficients obtained from the polynomial coefficients of Ref. [3] and from the polynomial coefficients obtained with all the measurements of this work is equal to (0.21 ± 2.34) %. Taking into account that in the present work the spectra were recorded with a pressure higher than in Ref. [3], the accuracy of the self–broadening coefficients should be better in this work. The accuracy of the calculated self–broadening coefficients, until $|m| = 27$, is estimated to be better than 5 %.

4.4. Self-shifting coefficients

The self-shifting coefficients have been measured for about 500 transitions. They are presented in the last column of the Tables 2-5. Despite of the fact that in the 1.9-μm spectral region the rotational dependence of these coefficients can be observed for most intense bands (see Figs. 8-9), it is found very difficult to model this dependence with enough accuracy. A mean value for the self-shifting coefficients of about -0.01cm^{-1}·atm^{-1} can be deduced from all the measurements in this region plotted in Fig. 10. In the 1.7-μm spectral region, no rotational dependence of the self-shifting coefficients (see Fig. 11) has been observed. All self-shifting coefficients measured in this region are presented in the Fig. 12 and the same mean value of -0.010cm^{-1}.atm^{-1} has been found with 1SD = 0.004cm^{-1}.atm^{-1}. It should be emphasized that this mean value is twice larger than that obtained in Ref. [3] for the 5-μm spectral region. Such an increase of the self-shifting coefficients with increasing energy levels has already been observed for other molecules, for example, CH_4 [28], and H_2O [29].

5. Conclusion

In this work, absolute line positions, line intensities and self-broadening and -shifting coefficients have been measured for about 550 transitions belonging to 13 bands of acetylene $^{12}C_2H_2$ between 5000 and 6000 cm^{-1}. The measured line intensities have been modeled using two different approaches: a semi-empirical approach involving vibrational transition dipole moment squared and the Herman-Wallis coefficients, and a global effective operators approach. An empirical polynomial expansion is proposed to describe the rotational dependence of the self-broadening coefficients of acetylene, and a mean value for the self-shifting coefficients in this spectral region has been deduced. The full set of measured line parameters is presented as Supplementary materials.

Acknowledgments

O.M.L. acknowledges a financial support by the Mairie of Paris (Bourse of Mairie of Paris for 2006).

References

[1] Mandin JY, Dana V, Claveau C. Line intensities in the ν_5 band of acetylene $^{12}C_2H_2$. JQSRT 2000;67:429-46.

[2] Jacquemart D, Claveau C, Mandin JY, Dana V. Line intensities of hot bands in the 13.6-μm spectral region of acetylene $^{12}C_2H_2$. JQSRT 2001;69:81-101.

[3] Jacquemart D, Mandin JY, Dana V, Régalia-Jarlot L, Thomas X, Von Der Heyden. Multispectrum fitting measurements of line parameters for 5-μm cold bands of acetylene. JQSRT 2002;75:397-422.

[4] Jacquemart D, Mandin JY, Dana V, Régalia-Jarlot L, Plateaux JJ, Décatoire D, Rothman LS. The spectrum of acetylene in the 5-μm region from new line parameter measurements. JQSRT 2003;76:237-67.

[5] Mandin JY, Jacquemart D, Dana V, Régalia-Jarlot L, Barbe A. Line intensities of acetylene at 3 μm. JQSRT 2005;92:239-60.

[6] Lyulin OM, Perevalov VI, Mandin JY, Dana V, Jacquemart D, Régalia-Jarlot L, Barbe A. Line intensities of acetylene in the 3-μm region: new measurements of weak hot bands and global fitting. JQSRT 2006;97:81–98.

[7] Jacquemart D, Lacome N, Mandin JY, Dana V, Lyulin OM, Perevalov VI. Multispectrum fitting of line parameters for $^{12}C_2H_2$ in the 3.8-μm spectral region. JQSRT 2007;103:478-95.

[8] Lyulin OM, Perevalov VI, Mandin JY, Dana V, Gueye F, Thomas X, Von der Heyden P, Décatoire D, Régalia-Jarlot L, Jacquemart D, Lacome N. Line intensities of acetylene: measurements in the 2.5-μm spectral region and global modelling in the ΔP=4 and 6 series. JQSRT 2007;103:496-523.

[9] Lyulin OM, Perevalov VI, Gueye F, Mandin JY, Dana V, Thomas X, Von Der Heyden P, Régalia-Jarlot L, Barbe A. Line positions and intensities of acetylene in the 2.2-μm region. JQSRT 2007;104:133-54.

[10] Vander Auwera J. Absolute intensities measurements in the $\nu_4 + \nu_5$ band of $^{12}C_2H_2$: Analysis of Herman–Wallis effects and forbidden transitions. J Mol Spectrosc 2000; 201:143-50.

[11] Vander Auwera J, Hurtmans D, Carleer M, Herman M. The ν_3 fundamental in C_2H_2: J Mol Spectrosc 1993;157:337–57.

[12] El Hachtouki R, Vander Auwera J. Absolute line intensities in acetylene: The 1.5 μm region. J Mol Spectrosc 2002;216:355-62.

[13] Smith BS, Winn JS. The C-H overtone spectra of acetylene: Band/stretch interactions below 10000cm^{-1}. J Chem Phys 1988;89:4638-45.

[14] Keppler KA, Mellau GCh, Klee S, Winnewisser BP, Winnewisser M, Pliva J, Narahari Rao K. Precision measurements of acetylene spectra at 1.4–1.7-μm recorded with 352.5-m pathlength. J Mol Spectrosc 1996;175:411-20.

[15] Jacquemart D, Mandin JY, Dana V, Picqué N, Guelachvili G. A multispectrum fitting procedure to deduce molecular line parameters. Application to the 3-0 band of $^{12}C^{16}O$. Eur Phys J D 2001;14:55-69.

[16] Wartewig S. IR and Raman Spectroscopy: Fundamental Processing. Wiley-VCH, Weinheim, 2003.

[17] Mertz L. Transformations in Optics. Wiley, New York, 1965.

[18] Griffiths PR, deHaseth JA. Fourier Transform Infrared Spectrometry. Wiley, New York, 1986.

[19] Lambot D, Olivier A, Blanquet G, Walrand J, Bouanich JP. Diode-laser measurements of collisional line broadening in the ν_5 band of C_2H_2. JQSRT 1991;45:145-55.

[20] Dicke RH. The effect of collisions upon the Doppler with of spectral lines. Phys.Rev. 1953;89:472-3.

[21] Gamache RR, Kennedy S, Hawkins RL, Rothman LS. Total internal partition sums for molecules in the terrestrial atmosphere. J Mol Struct 2000;517-8:407-25.

[22] Jacquemart D, Kwabia Tchana F, Lacome N, Kleiner I. A complete set of line parameters for CH_3Br in the 10-μm spectral region. JQSRT 2007;105:264-302.

[23] Lyulin OM, Perevalov VI, Teffo JL. Global fitting of the vibrational-rotational line positions of acetylene molecule in the far and middle infrared regions. In: Proceedings of the XIVth Symposium on High-Resolution Molecular Spectroscopy, Krasnoyarsk, Russia. SPIE 2004;5311:134-43.

[24] Perevalov VI, Lyulin OM, Jacquemart D, Claveau C, Teffo JL, Dana V, Mandin JY, Valentin A. Global fitting of line intensities of acetylene molecule in the infrared using the effective operator approach. J Mol Spectrosc 2003;218:180–9.

[25] Abbouti Temsamani M, Herman M. The vibrational energy levels in acetylene $^{12}C_2H_2$: Towards a regular pattern at higher energies. J Chem Phys 1995;102:6371-84.

[26] Rothman LS, Hawkins RL, Wattson RB, Gamache RR. Energy levels, intensities, and linewidths of atmospheric carbon dioxide bands. JQSRT 1992;48:537-66.

[27] Varanasi P, Giver LP, Valero FPJ. Infrared absorption by acetylene in the 12-14-μm region at low temperatures. JQSRT 1983;30:497-504.

[28] Predoi-Cross A, Brawley-Tremblay M, Brown LR, Malathy Devi V, Chris Benner D. Multispectrum analysis of $^{12}CH_4$ from 4100 to 4635 cm^{-1}: II. Air-broadening coefficients (widths and shifts). JQSRT 2006;236:201-15.

[29] Gamache RR, Hartmann JM. Collisional parameters of H_2O lines: effects of vibration. JQSRT 2004;83:119-47.

Captions of tables

Table 1. Experimental conditions and characteristics of the recorded spectra.

Table 2. Line parameters obtained for the $\nu_2 + \nu_3$ band of $^{12}C_2H_2$ [a].

Table 3. Line parameters obtained for the $\nu_1 + (2\nu_4 + \nu_5)^1I$ band of $^{12}C_2H_2$ [a].

Table 4. Line parameters obtained for the $\nu_2 + \nu_3 + \nu_4^1$ band of $^{12}C_2H_2$ [a].

Table 5. Line parameters obtained for the $\nu_1 + \nu_3 - \nu_4^1$ band of $^{12}C_2H_2$ [a].

Table 6. Fractions (squares of the expansion coefficients) of the principal basis functions in the case of J=3 for the upper states of the studied in the 1.9-μm region bands.

Table 7. Effective dipole moment parameters obtained as result of a simultaneous fit of all measured line intensities.

Table 8. Statistics of the simultaneous fit of all measured line intensities within the framework of the effective operators approach [a].

Table 9. Summary of vibrational transition dipole moments squared, and Herman-Wallis coefficients, obtained for the 13 bands analyzed in this work (see Eqs. (19-21)).

Table 10. Coefficients (in cm^{-1}/atm) of the empirical polynomial model used to reproduce the rotational dependence of the self-broadening coefficients.

Captions of figures

Fig. 1. Experimental (solid squares) and calculated (solid line) values of the transition dipole moment squared of the $\nu_2 + \nu_3$ band. The calculated values are obtained using the constants of Table 9.

Fig. 2. Experimental (squares for *P* and *R* branches and triangles for *Q* branch) and calculated (solid lines) values of the transition dipole moment squared of the $\nu_1 + (2\nu_4 + \nu_5)^1$I band. The calculated values of $|R|^2$ are obtained using the constants of Table 9.

Fig. 3. Experimental (squares for *P* and *R* branches and triangles for *Q* branch) and calculated (solid lines) values of the transition dipole moment squared of the $\nu_1 + \nu_3 - \nu_4^1$ band. The calculated values of $|R|^2$ are obtained using the constants of Table 9.

Fig. 4. Rotational dependence of the self-broadening coefficients for the $\nu_2 + \nu_3$ band.

Fig. 5. Rotational dependence of the self-broadening coefficients for the $\nu_1 + (2\nu_4 + \nu_5)^1$I band.

Fig. 6. Rotational dependence of the self-broadening coefficients for all measurements in the 1.9-μm region. The solid line is the polynomial fit of the whole set of these measurements and the triangles are the calculated self-broadening coefficients [3] in the 5-μm region.

Fig. 7. Rotational dependence of the self-broadening coefficients for all measurements in the 1.7-μm region. The solid line is the polynomial fit of the whole set of these measurements and the empty circles are the self-broadening coefficients calculated with the polynomial found in the 1.9-μm region.

Fig. 8. Self-shifting coefficients δ^0_{self} for the $\nu_2 + \nu_3$ band.

Fig. 9. Self-shifting coefficients δ^0_{self} for the $2\nu_2 + (\nu_4 + \nu_5)^0_+$ band.

Fig. 10. The whole set of the self-shifting coefficients δ^0_{self} measured in the 1.9-μm region.

Fig. 11. Self-shifting coefficients δ^0_{self} for the $\nu_2 + \nu_3 + \nu_4^1$ band.

Fig. 12. The whole set of the self-shifting coefficients δ^0_{self} measured in the 1.7-μm region.

Table 1. Experimental conditions and characteristics of the recorded spectra.

Unapodized *apparatus function*	
Maximum optical path difference	90 cm
Resolution (FWHM)	0.03 cm^{-1}
Nominal aperture radius	1 mm
Collimator focal length	418 mm
Absorbing sample	
Natural C_2H_2	97.760 % of $^{12}C_2H_2$
Stated purity	99.70 %
Experimental conditions	
SNR	≈ 100
Absorption path	1615 cm

#	Total pressure (mbar) [a]	Temperature (K)
1	35	297.85
2	79	297.45
3	125	298.35
4	180	298.15

[a] 1 atm = 1013 mbar = 1013 hPa.

Table 2. Line parameters obtained for the $\nu_2 + \nu_3$ band of $^{12}C_2H_2$ [a].

Line	Position	S_{obs}	S_{calc}	%S	$\|R\|^2_{obs}$	$\|R\|^2_{calc}$	%R	γ^0_{self}	δ^0_{self}
P29ee	5182.60776	4.55E-25	4.56E-25	-0.28	1.42E-07	1.36E-07	3.89	0.105	-0.020
P27ee	5188.51634	7.18E-25	7.94E-25	-10.54	1.25E-07	1.34E-07	-6.97	0.101	-0.011
P25ee	5194.35058	1.20E-24	1.31E-24	-9.28	1.23E-07	1.32E-07	-6.67	0.105	-0.010
P24ee	5197.23946	5.32E-25	5.52E-25	-3.65	1.28E-07	1.30E-07	-1.58	0.115	-0.016
P23ee	5200.10597	2.01E-24	2.06E-24	-2.50	1.28E-07	1.29E-07	-0.82	0.114	-0.011
P22ee	5202.95366	8.50E-25	8.45E-25	0.52	1.30E-07	1.28E-07	1.81	0.118	-0.013
P21ee	5205.77930	3.05E-24	3.08E-24	-0.73	1.27E-07	1.27E-07	0.25	0.121	-0.010
P20ee	5208.58510	1.20E-24	1.23E-24	-2.33	1.24E-07	1.26E-07	-1.64	0.122	-0.009
P19ee	5211.37002	4.14E-24	4.35E-24	-4.98	1.19E-07	1.25E-07	-4.57	0.122	-0.009
P18ee	5214.13303	1.61E-24	1.69E-24	-4.86	1.18E-07	1.24E-07	-4.71	0.124	-0.009
P17ee	5216.87623	6.22E-24	5.80E-24	6.71	1.31E-07	1.22E-07	6.61	0.138	
P16ee	5219.59271	2.21E-24	2.19E-24	1.01	1.22E-07	1.21E-07	0.69	0.136	
P15ee	5222.29083	7.39E-24	7.31E-24	1.14	1.21E-07	1.20E-07	0.62	0.136	-0.007
P14ee	5224.96638	2.71E-24	2.67E-24	1.32	1.20E-07	1.19E-07	0.62	0.141	-0.009
P13ee	5227.61873	8.60E-24	8.64E-24	-0.51	1.16E-07	1.18E-07	-1.38	0.140	-0.008
P12ee	5230.24943	3.08E-24	3.05E-24	0.82	1.17E-07	1.17E-07	-0.20	0.145	-0.011
P11ee	5232.85687	9.79E-24	9.54E-24	2.61	1.18E-07	1.16E-07	1.48	0.148	-0.008
P10ee	5235.44208	3.26E-24	3.24E-24	0.52	1.14E-07	1.15E-07	-0.75	0.149	-0.009
P 9ee	5238.00364	9.75E-24	9.72E-24	0.25	1.12E-07	1.14E-07	-1.13	0.150	-0.009
P 8ee	5240.54320	3.48E-24	3.16E-24	9.20	1.22E-07	1.13E-07	7.86	0.162	
P 7ee	5243.05919	9.12E-24	9.01E-24	1.29	1.11E-07	1.12E-07	-0.23	0.155	-0.007
P 6ee	5245.55259	2.79E-24	2.76E-24	1.19	1.10E-07	1.11E-07	-0.40	0.161	-0.007
P 5ee	5248.02210	7.40E-24	7.32E-24	1.07	1.09E-07	1.09E-07	-0.56	0.164	-0.005
P 4ee	5250.46784	2.02E-24	2.05E-24	-1.48	1.05E-07	1.08E-07	-3.18	0.166	-0.008
P 3ee	5252.89246	4.94E-24	4.78E-24	3.32	1.09E-07	1.07E-07	1.67	0.183	-0.005
P 2ee	5255.29295	1.14E-24	1.09E-24	4.85	1.10E-07	1.06E-07	3.22	0.196	
P 1ee	5257.66761	1.79E-24	1.66E-24	7.80	1.12E-07	1.05E-07	6.22	0.228	-0.008
	--								
R 0ee	5262.35478	5.85E-25	5.48E-25	6.42	1.08E-07	1.03E-07	4.85	0.209	-0.004
R 1ee	5264.65926	3.30E-24	3.22E-24	2.43	1.03E-07	1.02E-07	0.83	0.188	-0.007
R 2ee	5266.94199	1.60E-24	1.56E-24	2.49	1.02E-07	1.01E-07	0.93	0.179	-0.006
R 3ee	5269.20260	6.13E-24	5.97E-24	2.62	1.01E-07	1.00E-07	1.12	0.175	-0.010
R 5ee	5273.64951	8.45E-24	7.94E-24	6.04	1.03E-07	9.82E-08	4.73	0.162	-0.009
R 6ee	5275.83645	2.94E-24	2.86E-24	2.90	9.88E-08	9.72E-08	1.63	0.157	-0.010
R 7ee	5278.00139	8.99E-24	8.96E-24	0.30	9.53E-08	9.62E-08	-0.90	0.151	
R 8ee	5280.14337	3.13E-24	3.04E-24	2.88	9.69E-08	9.52E-08	1.82	0.151	-0.008
R 9ee	5282.26089	9.14E-24	9.06E-24	0.84	9.41E-08	9.42E-08	-0.12	0.146	-0.010
R10ee	5284.35482	2.93E-24	2.94E-24	-0.29	9.22E-08	9.32E-08	-1.11	0.146	-0.008
R11ee	5286.42560	8.58E-24	8.41E-24	2.03	9.35E-08	9.22E-08	1.38	0.144	-0.009
R13ee	5290.49668	7.36E-24	7.25E-24	1.47	9.14E-08	9.03E-08	1.15	0.141	-0.009
R14ee	5292.49803	2.19E-24	2.19E-24	0.18	8.94E-08	8.94E-08	0.05	0.142	-0.012
R15ee	5294.47312	6.22E-24	5.85E-24	6.01	9.42E-08	8.84E-08	6.10	0.139	-0.009
R16ee	5296.42825	1.78E-24	1.71E-24	3.93	9.13E-08	8.75E-08	4.23	0.132	-0.012
R17ee	5298.35897	4.34E-24	4.44E-24	-2.19	8.52E-08	8.65E-08	-1.61	0.125	-0.011
R19ee	5302.15234	3.00E-24	3.18E-24	-6.16	8.07E-08	8.47E-08	-4.97	0.121	-0.010
R20ee	5304.01432	8.44E-25	8.80E-25	-4.24	8.15E-08	8.37E-08	-2.74	0.122	-0.016
R21ee	5305.85404	2.12E-24	2.16E-24	-2.01	8.27E-08	8.28E-08	-0.19	0.120	-0.009
R22ee	5307.67531	5.40E-25	5.81E-25	-7.63	7.78E-08	8.19E-08	-5.33	0.109	-0.019
R23ee	5309.46899	1.26E-24	1.39E-24	-10.11	7.55E-08	8.10E-08	-7.32	0.110	-0.012
R24ee	5311.24578	3.57E-25	3.64E-25	-2.01	8.09E-08	8.01E-08	0.99	0.114	-0.020

[a] In the Line column, the first quoted character *e* or *f* concerns the upper level, and the second does the lower level. The position column contains the measured line position in cm^{-1}. S_{obs} is the measured line intensity in $cm \cdot molecule^{-1}$, for pure $^{12}C_2H_2$ at 296 K, and S_{calc} is that calculated using effective dipole moment parameters from the Table 7. $\%_S$ is the percentage ratio $100 \times (S_{obs} - S_{calc}) / S_{obs}$. $|R|^2_{obs}$ and $|R|^2_{calc}$ are the transition dipole moment squared in D^2 ($1\ D = 3.33546 \times 10^{-30}\ C \cdot m$), first is deduced from S_{obs} and second is calculated with Herman-Wallis coefficients from Table 9. $\%_R$ is the percentage ratio $100 \times (|R|^2_{obs} - |R|^2_{calc}) / |R|^2_{obs}$. γ^0_{self} and δ^0_{self} are the observed self-broadening and self-shifting coefficients in ($cm^{-1}.atm^{-1}$) respectively. Only the significant self-shifting coefficients are quoted.

Table 3. Line parameters obtained for the $\nu_1 + (2\nu_4 + \nu_5)^1$I band of $^{12}C_2H_2$ [a].

Line	Position	S_{obs}	S_{calc}	%S	$\|R\|^2_{obs}$	$\|R\|^2_{calc}$	%R	γ^0_{self}	δ^0_{self}
P19ee	5244.18361	7.26E-25	6.47E-25	10.93	4.39E-08	4.90E-08	-11.69	0.130	-0.006
P17ee	5248.98437	1.25E-24	1.10E-24	11.56	5.55E-08	5.61E-08	-1.07	0.142	-0.010
P15ee	5253.75944	1.92E-24	1.75E-24	9.00	6.70E-08	6.27E-08	6.39	0.143	-0.011
P14ee	5256.13763	7.31E-25	7.06E-25	3.53	6.94E-08	6.59E-08	5.03	0.147	
P13ee	5258.50874	2.60E-24	2.48E-24	4.68	7.58E-08	6.88E-08	9.17	0.150	-0.011
P12ee	5260.87230	1.01E-24	9.32E-25	8.08	8.34E-08	7.16E-08	14.12	0.153	-0.007
P10ee	5265.58800	9.88E-25	1.07E-24	-8.29	7.63E-08	7.66E-08	-0.42	0.152	-0.006
P 9ee	5267.94172	3.14E-24	3.27E-24	-4.03	8.11E-08	7.88E-08	2.88	0.154	-0.008
P 8ee	5270.29522	1.07E-24	1.07E-24	-0.45	8.52E-08	8.07E-08	5.26	0.158	-0.008
P 7ee	5272.64444	2.73E-24	3.05E-24	-11.68	7.74E-08	8.25E-08	-6.55	0.152	-0.008
P 6ee	5274.99481	9.61E-25	9.25E-25	3.75	9.04E-08	8.39E-08	7.10	0.164	-0.003
P 5ee	5277.34459	2.34E-24	2.39E-24	-2.05	8.56E-08	8.52E-08	0.48	0.172	-0.004
P 3ee	5282.04823	1.31E-24	1.33E-24	-1.46	8.65E-08	8.69E-08	-0.47	0.200	
	--								
R 1ee	5293.81347	2.08E-24	2.12E-24	-2.17	8.60E-08	8.65E-08	-0.65	0.198	-0.010
R 2ee	5296.16755	7.97E-25	9.21E-25	-15.53	7.60E-08	8.57E-08	-12.82	0.177	-0.005
R 3ee	5298.52431	3.28E-24	3.33E-24	-1.47	8.63E-08	8.46E-08	1.99	0.181	-0.009
R 4ee	5300.87962	1.29E-24	1.27E-24	1.67	8.88E-08	8.32E-08	6.22	0.173	-0.011
R 5ee	5303.23342	3.91E-24	4.17E-24	-6.65	8.14E-08	8.16E-08	-0.32	0.162	-0.009
R 6ee	5305.58798	1.46E-24	1.47E-24	-0.99	8.52E-08	7.98E-08	6.33	0.159	-0.010
R 7ee	5307.93983	4.22E-24	4.53E-24	-7.31	7.91E-08	7.77E-08	1.73	0.153	-0.009
R 8ee	5310.28996	1.43E-24	1.50E-24	-4.83	7.93E-08	7.54E-08	4.92	0.155	-0.008
R 9ee	5312.63648	4.33E-24	4.34E-24	-0.12	8.06E-08	7.29E-08	9.52	0.154	-0.009
R10ee	5314.97749	1.25E-24	1.35E-24	-8.03	7.16E-08	7.02E-08	1.88	0.147	-0.009
R11ee	5317.31398	3.62E-24	3.65E-24	-0.73	7.24E-08	6.74E-08	6.98	0.154	-0.008
R14ee	5324.28024	7.71E-25	7.32E-25	5.03	5.87E-08	5.78E-08	1.45	0.144	-0.012
R15ee	5326.58284	1.89E-24	1.76E-24	6.76	5.35E-08	5.44E-08	-1.65	0.145	-0.005
R16ee	5328.88081	5.42E-25	4.63E-25	14.70	5.22E-08	5.08E-08	2.66	0.134	-0.007
R20ee	5338.01702	1.88E-25	1.61E-25	14.52	3.44E-08	3.62E-08	-4.97	0.120	-0.013
R21ee	5340.28510	4.36E-25	3.63E-25	16.76	3.23E-08	3.25E-08	-0.37	0.123	-0.017
	--								
Q 7fe	5288.96868	7.98E-24	7.99E-24	-0.09	9.01E-08	8.75E-08	2.87	0.157	-0.010
Q11fe	5288.74739	6.99E-24	7.95E-24	-13.66	7.95E-08	8.75E-08	-10.02	0.145	-0.013
Q13fe	5288.58732	7.11E-24	6.95E-24	2.37	9.17E-08	8.75E-08	4.60	0.147	-0.005
Q15fe	5288.38809	5.54E-24	5.64E-24	-1.84	8.66E-08	8.75E-08	-0.98	0.143	
Q16fe	5288.27551	1.74E-24	1.65E-24	4.86	9.20E-08	8.75E-08	4.89	0.146	-0.015
Q17fe	5288.15127	4.38E-24	4.30E-24	1.89	8.85E-08	8.75E-08	1.13	0.136	-0.012
Q18fe	5288.01684	1.20E-24	1.22E-24	-2.18	8.43E-08	8.75E-08	-3.78	0.131	-0.013
Q19fe	5287.87064	2.86E-24	3.09E-24	-8.22	7.90E-08	8.75E-08	-10.69	0.122	-0.007
Q20fe	5287.71798	8.31E-25	8.56E-25	-3.07	8.25E-08	8.75E-08	-6.09	0.120	-0.010
Q21fe	5287.55086	2.13E-24	2.11E-24	1.20	8.56E-08	8.75E-08	-2.24	0.125	-0.013
Q22fe	5287.37406	5.33E-25	5.69E-25	-6.84	7.88E-08	8.75E-08	-11.06	0.121	-0.009
Q23fe	5287.18656	1.51E-24	1.37E-24	9.40	9.26E-08	8.75E-08	5.49	0.122	-0.009
Q25fe	5286.78078	8.57E-25	8.44E-25	1.55	8.48E-08	8.75E-08	-3.16	0.116	-0.016
Q27fe	5286.33137	4.83E-25	4.96E-25	-2.75	8.11E-08	8.75E-08	-7.85	0.102	-0.010

[a] See footnote of Table 2 for the meaning of column headings.

Table 4. Line parameters obtained for the $\nu_2 + \nu_3 + \nu_4{}^1$ band of $^{12}C_2H_2$ [a].

Line	Position	S_{obs}	S_{calc}	%S	$\|R\|^2_{obs}$	$\|R\|^2_{calc}$	%R	γ^0_{self}	δ^0_{self}
Pee23	5789.95823	1.10E-24	1.05E-24	4.91	1.31E-07	1.28E-07	2.88	0.119	-0.010
Pee22	5792.86730	4.14E-25	4.33E-25	-4.62	1.20E-07	1.27E-07	-6.10	0.122	-0.012
Pee21	5795.75287	1.54E-24	1.59E-24	-3.39	1.21E-07	1.26E-07	-4.29	0.120	-0.010
Pee20	5798.61738	6.61E-25	6.40E-25	3.30	1.29E-07	1.25E-07	2.86	0.134	-0.010
Pee19	5801.45957	2.26E-24	2.28E-24	-1.00	1.23E-07	1.25E-07	-1.14	0.135	-0.018
Pee18	5804.27696	9.37E-25	8.89E-25	5.11	1.31E-07	1.24E-07	5.21	0.143	-0.012
Pee17	5807.06843	2.94E-24	3.07E-24	-4.40	1.18E-07	1.23E-07	-4.09	0.137	-0.008
Pee15	5812.58177	3.88E-24	3.89E-24	-0.23	1.22E-07	1.22E-07	0.31	0.141	-0.008
Pee13	5817.99420	4.77E-24	4.60E-24	3.56	1.26E-07	1.20E-07	4.21	0.134	-0.010
Pee12	5820.66505	1.68E-24	1.62E-24	3.33	1.25E-07	1.20E-07	4.02	0.151	-0.012
Pee11	5823.30575	4.85E-24	5.04E-24	-4.08	1.15E-07	1.19E-07	-3.30	0.147	-0.007
Pee10	5825.92245	1.75E-24	1.71E-24	2.56	1.22E-07	1.18E-07	3.31	0.159	-0.009
Pee 9	5828.51439	5.02E-24	5.08E-24	-1.11	1.17E-07	1.17E-07	-0.32	0.155	-0.009
Pee 8	5831.07998	1.58E-24	1.63E-24	-3.22	1.14E-07	1.17E-07	-2.39	0.161	-0.009
Pee 7	5833.61776	4.39E-24	4.57E-24	-4.16	1.12E-07	1.16E-07	-3.32	0.151	-0.007
Pee 5	5838.61691	3.39E-24	3.50E-24	-3.10	1.12E-07	1.15E-07	-2.26	0.169	-0.006
Pee 4	5841.07685	8.81E-25	9.20E-25	-4.48	1.10E-07	1.14E-07	-3.62	0.179	-0.008
Pee 3	5843.50900	2.04E-24	1.92E-24	6.12	1.22E-07	1.13E-07	6.89	0.197	-0.010
	--								
Ree 1	5855.27558	2.91E-24	2.96E-24	-1.60	1.09E-07	1.10E-07	-0.73	0.193	-0.009
Ree 2	5857.54810	1.20E-24	1.28E-24	-6.23	1.04E-07	1.09E-07	-5.30	0.180	-0.004
Ree 3	5859.79506	4.51E-24	4.60E-24	-1.90	1.07E-07	1.08E-07	-1.00	0.173	-0.009
Ree 4	5862.01346	1.71E-24	1.75E-24	-2.18	1.06E-07	1.08E-07	-1.27	0.167	-0.009
Ree 6	5866.37407	2.08E-24	2.03E-24	2.45	1.10E-07	1.06E-07	3.33	0.161	-0.016
Ree 7	5868.51164	6.10E-24	6.29E-24	-3.01	1.03E-07	1.06E-07	-2.07	0.153	-0.009
Ree 9	5872.70927	6.14E-24	6.25E-24	-1.74	1.03E-07	1.04E-07	-0.82	0.151	-0.005
Ree10	5874.76942	2.00E-24	2.01E-24	-0.81	1.04E-07	1.04E-07	0.09	0.145	-0.012
Ree11	5876.80094	5.81E-24	5.74E-24	1.27	1.05E-07	1.03E-07	2.13	0.148	-0.009
Ree12	5878.80647	1.87E-24	1.78E-24	4.85	1.08E-07	1.02E-07	5.64	0.150	-0.010
Ree13	5880.78676	4.91E-24	4.91E-24	-0.02	1.02E-07	1.02E-07	0.74	0.141	-0.010
Ree14	5882.74030	1.42E-24	1.48E-24	-4.22	9.75E-08	1.01E-07	-3.52	0.137	-0.008
Ree15	5884.66838	3.96E-24	3.93E-24	0.75	1.02E-07	1.00E-07	1.30	0.138	-0.012
Ree16	5886.57002	1.17E-24	1.15E-24	1.54	1.02E-07	9.96E-08	1.92	0.136	-0.010
Ree17	5888.44636	2.97E-24	2.97E-24	0.33	9.94E-08	9.89E-08	0.49	0.129	-0.010
Ree18	5890.29764	8.03E-25	8.39E-25	-4.47	9.39E-08	9.83E-08	-4.62	0.123	-0.008
Ree21	5895.70938	1.48E-24	1.41E-24	5.12	9.98E-08	9.63E-08	3.45	0.123	-0.022
Ree23	5899.20161	8.75E-25	8.85E-25	-1.12	9.04E-08	9.50E-08	-5.11	0.115	-0.019
	--								
Qfe 3	5850.56150	6.27E-24	6.59E-24	-5.16	1.07E-07	1.11E-07	-4.32	0.179	-0.010
Qfe 5	5850.42818	9.25E-24	9.33E-24	-0.94	1.11E-07	1.11E-07	-0.21	0.161	-0.011
Qfe 6	5850.33959	3.71E-24	3.43E-24	7.42	1.21E-07	1.11E-07	8.05	0.177	-0.015
Qfe 7	5850.23655	1.14E-23	1.10E-23	3.89	1.16E-07	1.11E-07	4.49	0.159	-0.010
Qfe 8	5850.11852	3.90E-24	3.77E-24	3.19	1.15E-07	1.11E-07	3.73	0.167	-0.008
Qfe 9	5849.98662	1.15E-23	1.14E-23	0.62	1.12E-07	1.11E-07	1.09	0.151	-0.007
Qfe10	5849.84103	3.84E-24	3.75E-24	2.39	1.14E-07	1.11E-07	2.76	0.147	-0.008
Qfe11	5849.67976	1.08E-23	1.08E-23	-0.27	1.11E-07	1.11E-07	0.00	0.147	-0.010
Qfe12	5849.50529	3.43E-24	3.42E-24	0.25	1.12E-07	1.11E-07	0.39	0.143	-0.012
Qfe13	5849.31602	9.89E-24	9.53E-24	3.64	1.15E-07	1.11E-07	3.64	0.140	-0.007
Qfe14	5849.11457	3.02E-24	2.90E-24	3.91	1.15E-07	1.11E-07	3.75	0.145	-0.010
Qfe15	5848.89742	7.92E-24	7.83E-24	1.09	1.12E-07	1.11E-07	0.75	0.138	-0.009
Qfe16	5848.66779	2.35E-24	2.31E-24	1.73	1.12E-07	1.11E-07	1.19	0.137	-0.011
Qfe17	5848.42459	6.02E-24	6.04E-24	-0.33	1.10E-07	1.11E-07	-1.12	0.131	-0.008
Qfe18	5848.17002	1.84E-24	1.73E-24	5.95	1.17E-07	1.11E-07	4.95	0.135	-0.015
Qfe19	5847.89993	4.34E-24	4.38E-24	-0.96	1.09E-07	1.11E-07	-2.33	0.124	-0.010
Qfe22	5847.02190	8.33E-25	8.11E-25	2.59	1.11E-07	1.11E-07	0.16	0.122	-0.018
Qfe23	5846.70174	1.91E-24	1.95E-24	-2.06	1.06E-07	1.11E-07	-5.11	0.117	-0.010
Qfe25	5846.03434	1.15E-24	1.19E-24	-4.10	1.03E-07	1.11E-07	-8.39	0.108	-0.009

[a] See footnote of Table 3 for the meaning of column headings.

Table 5. Line parameters obtained for the $\nu_1 + \nu_3 - \nu_4^1$ band of $^{12}C_2H_2$ [a].

Line	Position	S_{obs}	S_{calc}	%S	$\|R\|^2_{obs}$	$\|R\|^2_{calc}$	%R	γ^0_{self}	δ^0_{self}
Pee23	5884.95417	5.57E-25	5.70E-25	-2.43	1.17E-06	1.20E-06	-2.36	0.118	-0.024
Pee21	5890.62433	8.40E-25	8.55E-25	-1.76	1.15E-06	1.17E-06	-1.71	0.122	-0.008
Pee19	5896.20887	1.19E-24	1.22E-24	-2.19	1.12E-06	1.15E-06	-2.15	0.129	-0.008
Pee17	5901.70399	1.65E-24	1.63E-24	1.05	1.13E-06	1.12E-06	1.09	0.134	-0.009
Pee16	5904.41880	6.58E-25	6.17E-25	6.17	1.18E-06	1.11E-06	6.21	0.142	-0.017
Pee15	5907.10958	2.21E-24	2.07E-24	6.28	1.17E-06	1.10E-06	6.31	0.144	-0.010
Pee14	5909.78006	6.99E-25	7.59E-25	-8.64	9.97E-07	1.08E-06	-8.61	0.138	-0.006
Pee13	5912.42611	2.48E-24	2.47E-24	0.59	1.08E-06	1.07E-06	0.62	0.152	-0.015
Pee12	5915.05069	8.83E-25	8.76E-25	0.86	1.07E-06	1.06E-06	0.88	0.155	-0.009
Pee11	5917.65283	2.76E-24	2.75E-24	0.50	1.05E-06	1.05E-06	0.52	0.153	-0.010
Pee 9	5922.78894	2.80E-24	2.85E-24	-1.70	1.00E-06	1.02E-06	-1.69	0.155	-0.010
Pee 8	5925.32178	9.57E-25	9.36E-25	2.22	1.03E-06	1.01E-06	2.24	0.155	-0.009
Pee 7	5927.83355	2.68E-24	2.70E-24	-0.92	9.89E-07	9.98E-07	-0.90	0.160	-0.010
Pee 6	5930.32162	8.19E-25	8.44E-25	-3.10	9.56E-07	9.86E-07	-3.09	0.172	-0.008
Pee 5	5932.78730	2.30E-24	2.30E-24	-0.05	9.74E-07	9.74E-07	-0.04	0.176	-0.010
Pee 3	5937.64985	1.65E-24	1.66E-24	-0.45	9.46E-07	9.51E-07	-0.44	0.194	-0.010
Pee 1	5942.42083	8.82E-25	8.57E-25	2.84	9.55E-07	9.27E-07	2.85	0.209	-0.010
	--								
Ree 3	5953.94167	1.16E-24	1.14E-24	1.52	8.84E-07	8.71E-07	1.53	0.189	-0.005
Ree 5	5958.38897	1.68E-24	1.68E-24	0.21	8.50E-07	8.48E-07	0.23	0.170	-0.007
Ree 6	5960.57693	6.42E-25	6.18E-25	3.71	8.70E-07	8.37E-07	3.72	0.161	
Ree 9	5966.99963	1.89E-24	2.03E-24	-7.79	7.47E-07	8.05E-07	-7.77	0.146	-0.002
Ree10	5969.09617	6.86E-25	6.63E-25	3.33	8.22E-07	7.94E-07	3.36	0.152	-0.017
Ree11	5971.16776	2.00E-24	1.91E-24	4.68	8.22E-07	7.84E-07	4.71	0.156	-0.010
Ree12	5973.21479	5.87E-25	5.96E-25	-1.64	7.61E-07	7.73E-07	-1.61	0.143	-0.005
Ree13	5975.24093	1.51E-24	1.65E-24	-9.30	6.98E-07	7.63E-07	-9.27	0.112	-0.010
Ree15	5979.21538	1.38E-24	1.33E-24	3.52	7.69E-07	7.42E-07	3.55	0.143	-0.009
Ree17	5983.09943	1.04E-24	1.01E-24	2.99	7.44E-07	7.21E-07	3.04	0.133	-0.012
Ree19	5986.88671	6.83E-25	7.17E-25	-4.95	6.68E-07	7.01E-07	-4.89	0.107	-0.007
Ree21	5990.58038	4.98E-25	4.83E-25	3.15	7.04E-07	6.81E-07	3.21	0.122	-0.010
	--								
Qef 2	5944.66959	2.25E-24	2.07E-24	7.92	9.95E-07	9.16E-07	7.92	0.203	-0.010
Qef 3	5944.57010	1.01E-24	9.33E-25	7.73	9.93E-07	9.16E-07	7.73	0.189	-0.006
Qef 4	5944.43552	3.39E-24	3.44E-24	-1.41	9.03E-07	9.16E-07	-1.40	0.175	-0.011
Qef 5	5944.26953	1.33E-24	1.32E-24	0.90	9.24E-07	9.16E-07	0.90	0.168	-0.016
Qef 6	5944.06636	4.39E-24	4.37E-24	0.44	9.20E-07	9.16E-07	0.43	0.164	-0.012
Qef 7	5943.83166	1.47E-24	1.55E-24	-5.33	8.69E-07	9.16E-07	-5.34	0.156	-0.008
Qef 8	5943.56307	4.80E-24	4.82E-24	-0.28	9.13E-07	9.16E-07	-0.29	0.155	-0.009
Qef 9	5943.26148	1.64E-24	1.62E-24	1.53	9.30E-07	9.16E-07	1.52	0.154	-0.015
Qef10	5942.92632	4.70E-24	4.78E-24	-1.75	9.00E-07	9.16E-07	-1.77	0.150	-0.009
Qef11	5942.55691	1.54E-24	1.54E-24	-0.11	9.15E-07	9.16E-07	-0.14	0.148	-0.009
Qef12	5942.15546	4.39E-24	4.37E-24	0.30	9.18E-07	9.16E-07	0.27	0.147	-0.007
Qef13	5941.71951	1.34E-24	1.36E-24	-1.24	9.04E-07	9.16E-07	-1.28	0.142	-0.010
Qef14	5941.25101	3.59E-24	3.72E-24	-3.51	8.84E-07	9.16E-07	-3.57	0.138	-0.009
Qef16	5940.21243	2.88E-24	2.96E-24	-3.02	8.88E-07	9.16E-07	-3.10	0.134	-0.010
Qef19	5938.40721	6.23E-25	6.28E-25	-0.94	9.06E-07	9.16E-07	-1.05	0.131	-0.014
Qef20	5937.73707	1.55E-24	1.58E-24	-1.38	9.02E-07	9.16E-07	-1.51	0.122	-0.008
Qef22	5936.30105	1.09E-24	1.06E-24	3.41	9.47E-07	9.16E-07	3.26	0.118	-0.013
Qef24	5934.73103	7.04E-25	6.70E-25	4.75	9.60E-07	9.16E-07	4.57	0.114	-0.019

[a] See footnote of Table 3 for the meaning of column headings.

Table 6. Fractions (squares of the expansion coefficients) of the principal basis functions in the case of J=3 for the upper states of the studied in the 1.9μm region bands.

Bands		Basis functions (notation $V_1V_2V_3V_4V_5\ \ell_4\ell_5$)								
		01100 00	02011 1-1	00130 10	01041 2-1	10021 2-1	10021 01	01023 2-1	01023 01	10003 01
Eigenfunctions of the upper states	$\nu_2 + \nu_3$	0.90	0.09							
	$2\nu_2 + (\nu_4 + \nu_5)^0_+$	0.09	0.90							
	$\nu_3 + 3\nu_4{}^1$			0.48	0.32					
	$\nu_2 + (4\nu_4 + \nu_5)^1$II			0.50	0.36					
	$\nu_1 + (2\nu_4 + \nu_5)^1$I					0.44	0.30			
	$\nu_2 + (2\nu_4 + 3\nu_5)^1$III						0.29	0.23	0.23	
	$\nu_1 + 3\nu_5{}^1$									0.98

Table 7. Effective dipole moment parameters obtained as result of a simultaneous fit of all measured line intensities.

Parameter[a]	ΔV_1	ΔV_2	ΔV_3	ΔV_4	ΔV_5	$\Delta \ell_4$	$\Delta \ell_5$	Value[b]	Order
$\Delta P=8$									
M	0	1	1	0	0	0	0	2.16(1)	10^{-4}
b_J	0	1	1	0	0	0	0	-6.1(4)	10^{-3}
M	0	2	0	1	1	1	-1	-9.38(3)	10^{-5}
b_J	0	2	0	1	1	1	-1	-3.5(2)	10^{-3}
M	0	0	1	3	0	1	0	-0.4(2)	10^{-6}
d_{JQ}	0	0	1	3	0	1	0	0.3(2)	10^{-1}
M	0	1	0	4	1	2	-1	-1.600(8)	10^{-5}
b_J	0	1	0	4	1	2	-1	-7.2(3)	10^{-3}
d_{JQ}	0	1	0	4	1	2	-1	-1.4(3)	10^{-4}
M	1	0	0	2	1	0	1	1.217(6)	10^{-4}
M	0	1	0	2	3	2	-1	-1.09(2)	10^{-5}
b_J	0	1	0	2	3	2	-1	1.01(9)	10^{-2}
M	1	0	0	0	3	0	1	-2.23 (1)	10^{-5}
$\Delta P=9$									
M	0	1	1	1	0	1	0	-1.409(5)	10^{-4}
b_J	0	1	1	1	0	1	0	-3.5(3)	10^{-3}
M	0	2	0	2	1	2	-1	4.02(1)	10^{-5}
b_J	0	2	0	2	1	2	-1	-1.8(3)	10^{-3}
M	1	0	1	-1	0	1	0	4.96(1)	10^{-4}
b_J	1	0	1	-1	0	1	0	-6.2(3)	10^{-3}
M	0	0	2	0	-1	0	1	4.46(1)	10^{-4}
b_J	0	0	2	0	-1	0	1	-4.5(4)	10^{-3}
M	1	1	0	2	-1	0	1	6.7(1)	10^{-5}
M	2	0	0	0	-1	0	1	4.56(1)	10^{-4}
b_J	2	0	0	0	-1	0	1	-6.4(4)	10^{-3}

[a]Parameters M are given in debye (1D = 3.33546×10^{-30} C·m), while the other parameters are dimensionless.
[b]Confidence intervals (1 SD, in unit of the last quoted digit) are given between parenthesis.

Table 8. Statistics of the simultaneous fit of all measured line intensities within the framework of the effective operators approach [a].

Band	Region(cm^{-1})	J_{max}	N_b	MR(%)	RMS(%)
$\Delta P=8$					
$\nu_2 + \nu_3$	5182.6-5314.7	29	49	0.17	4.32
$2\nu_2 + (\nu_4 + \nu_5)^0{}_+$	5159.8-5282.5	29	47	0.27	5.05
$\nu_3 + 3\nu_4{}^1$	5048.7-5147.4	25	49	0.63	7.24
$\nu_2 + (4\nu_4 + \nu_5)^1$II	5077.2-5164.1	25	47	0.20	5.79
$\nu_1 + (2\nu_4 + \nu_5)^1$I	5244.2-5344.8	27	43	0.41	7.38
$\nu_2 + (2\nu_4 + 3\nu_5)^1$III	5249.9-5358.9	25	45	0.53	6.31
$\nu_1 + 3\nu_5{}^1$	5462.8-5566.5	25	45	0.30	5.33
$\Delta P=9$					
$\nu_2 + \nu_3 + \nu_4{}^1$	5790.0- 5899.2	25	55	0.13	3.39
$2\nu_2 + (2\nu_4 + \nu_5)^1$II	5773.7- 5858.8	23	26	0.21	4.80
$\nu_1+ \nu_3 - \nu_4{}^1$	5885.0- 5990.6	24	47	0.14	3.77
$2\nu_3 - \nu_5{}^1$	5722.0- 5805.9	23	34	0.20	4.66
$\nu_1 + \nu_2 + 2\nu_4{}^0 - \nu_5{}^1$	5734.7- 5822.2	21	30	0.15	3.68
$2\nu_1 - \nu_5{}^1$	5944.5- 6011.9	21	28	0.13	3.62

[a] J_{max} is the maximum value of the rotational quantum number in the file of the observed data, N_b is the number of measured line intensities, MR (%) is the mean value of the residuals, RMS (%) is the root mean square of the residuals.

Table 9. Summary of vibrational transition dipole moments squared, and Herman-Wallis coefficients, obtained for the 13 bands analyzed in this work (see Eqs. (19-21)).

Center[a]	Band	Vibrational symmetry	Number of transitions	$\|R_0\|^2$ (in 10^{-8} D^2)[b]	A_1^{RP} (in 10^{-3})	A_2^{RP} (in 10^{-4})	A_2^{Q} (in 10^{-4})
5260.02	$\nu_2 + \nu_3$	$\Sigma^+_u \leftarrow \Sigma^+_g$	50	10.42(5)[c]	-4.9(2)	0	0
5230.23	$2\nu_2 + (\nu_4 + \nu_5)^0_+$	$\Sigma^+_u \leftarrow \Sigma^+_g$	42	8.32(6)	–2.6(2)	0	0
5102.80	$\nu_3 + 3\nu_4^1$	$\Pi_u \leftarrow \Sigma^+_g$	43	5.16(5)	–5.9(3)	-2.7(2)	0
5124.57	$\nu_2 + (4\nu_4 + \nu_5)^1$II	$\Pi_u \leftarrow \Sigma^+_g$	38	3.73(5)	-4.8(3)	–2.3(3)	-1.9(2)
5290.28	$\nu_1 + (2\nu_4 + \nu_5)^1$I	$\Pi_u \leftarrow \Sigma^+_g$	43	8.7(1)	–1.1(4)	-7.6(3)	0
5302.30	$\nu_2 + (2\nu_4 + 3\nu_5)^1$III	$\Pi_u \leftarrow \Sigma^+_g$	38	3.35(5)	–5.4(5)	2.5(3)	-3.0(4)
5510.40	$\nu_1 + 3\nu_5^1$	$\Pi_u \leftarrow \Sigma^+_g$	46	2.22(1)	–2.0(3)	0	0
5849.47	$\nu_2 + \nu_3 + \nu_4^1$	$\Pi_u \leftarrow \Sigma^+_g$	55	11.11(6)	-3.1(2)	0	0
5815.69	$2\nu_2 + (2\nu_4 + \nu_5)^1$II	$\Pi_u \leftarrow \Sigma^+_g$	26	2.76(2)	–1.6(3)	0	0
5945.93	$\nu_1 + \nu_3 - \nu_4^1$	$\Sigma^+_u \leftarrow \Pi_g$	47	91.6(5)	–6.3(3)	0	0
5774.24	$2\nu_3 - \nu_5^1$	$\Sigma^+_g \leftarrow \Pi_u$	34	120.3(10)	-5.2(5)	0	0
5786.00	$\nu_1 + \nu_2 + 2\nu_4^0 - \nu_5^1$	$\Sigma^+_g \leftarrow \Pi_u$	30	118.6(15)	–4.7(5)	-3.8(4)	-3.9(3)
5981.03	$2\nu_1 - \nu_5^1$	$\Sigma^+_g \leftarrow \Pi_u$	28	78.7(6)	–7.2(5)	0	0

[a] Rough values of band centers (in cm^{-1}) are reported only as a guide.
[b] 1 debye = 3.33546×10^{-30} C·m.
[c] Confidence intervals (1 SD, in unit of the last quoted digit) are given between parenthesis.

Table 10. Coefficients (in cm^{-1}/atm) of the empirical polynomial model used to reproduce the rotational dependence of the self-broadening coefficients.

	A_0	B_1	B_2	B_3	B_4	B_5
1.9-μm	0.226	-0.0211	0.00253	-1.537×10^{-4}	4.26×10^{-6}	-4.4×10^{-8}
1.7-μm	0.215	-0.0134	0.00115	-0.506×10^{-4}	0.78×10^{-6}	
All data	0.222	-0.0184	0.00206	-1.212×10^{-4}	3.24×10^{-6}	-3.17×10^{-8}

Fig. 1. Experimental (solid squares) and calculated (solid line) values of the transition dipole moment squared of the $\nu_2 + \nu_3$ band. The calculated values are obtained using the constants of Table 9.

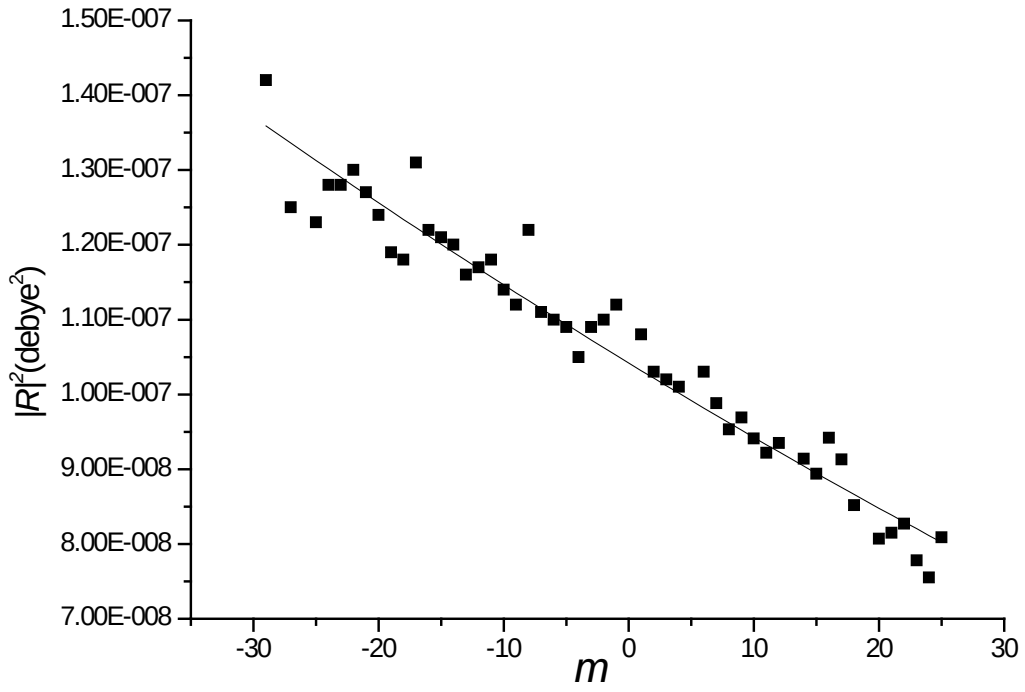

Fig. 2. Experimental (squares for *P* and *R* branches and triangles for *Q* branch) and calculated (solid lines) values of the transition dipole moment squared of the $\nu_1 + (2\nu_4 + \nu_5)^1$I band. The calculated values of $|R|^2$ are obtained using the constants of Table 9.

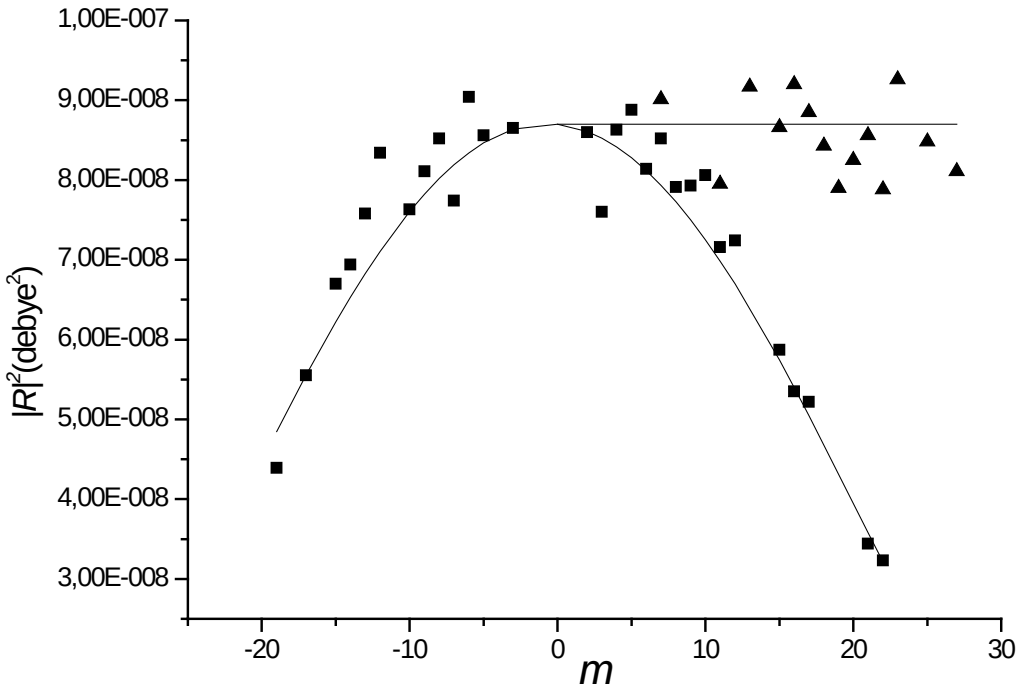

Fig. 3. Experimental (squares for *P* and *R* branches and triangles for *Q* branch) and calculated (solid lines) values of the transition dipole moment squared of the $\nu_1 + \nu_3 - \nu_4^1$ band. The calculated values of $|R|^2$ are obtained using the constants of Table 9.

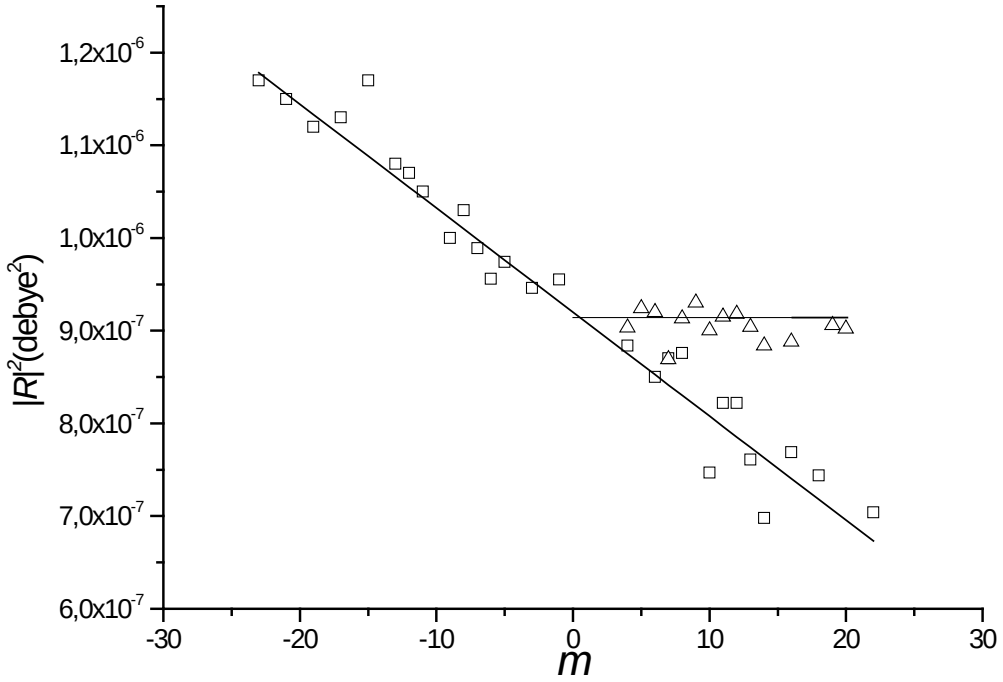

Fig. 4. Rotational dependence of the self-broadening coefficients for the $\nu_2 + \nu_3$ band.

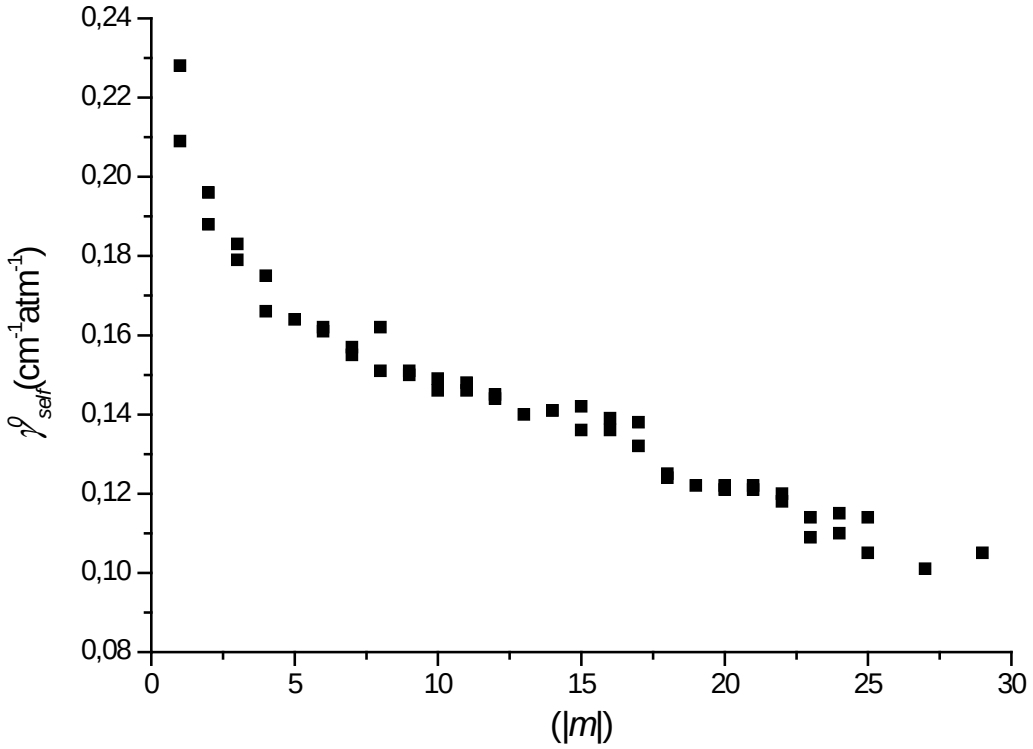

Fig. 5. Rotational dependence of the self-broadening coefficients for the $\nu_1 + (2\nu_4 + \nu_5)^1$I band.

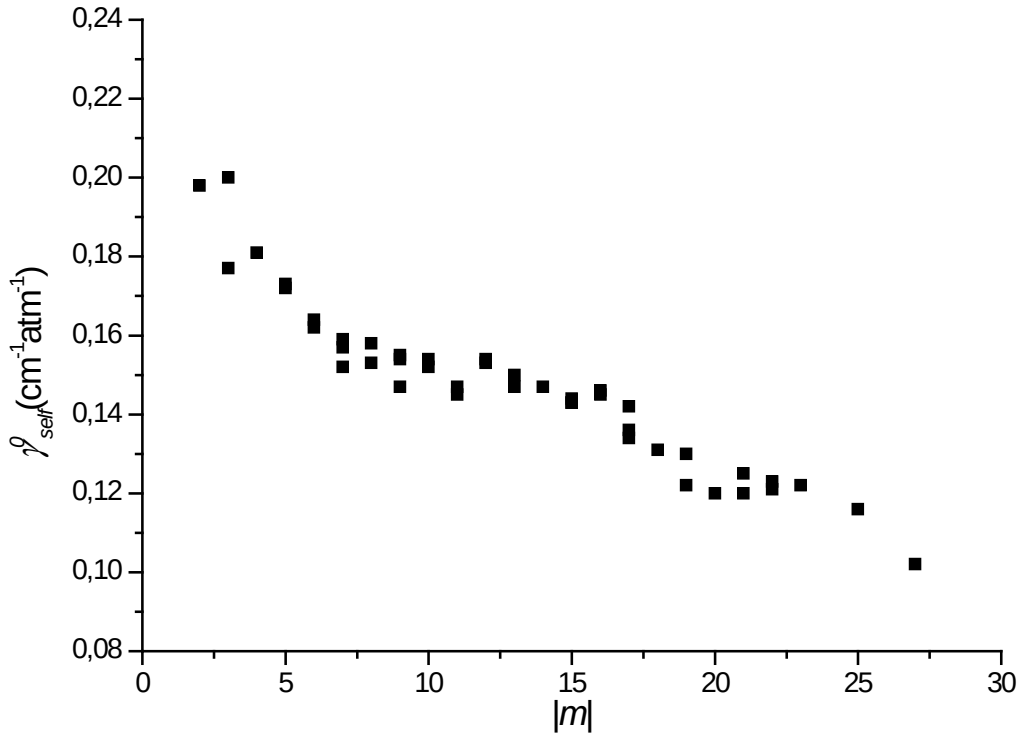

Fig. 6. Rotational dependence of the self-broadening coefficients for all measurements in the 1.9-μm region. The solid line is the polynomial fit of the whole set of these measurements and the triangles are the calculated self-broadening coefficients [3] in the 5-μm region.

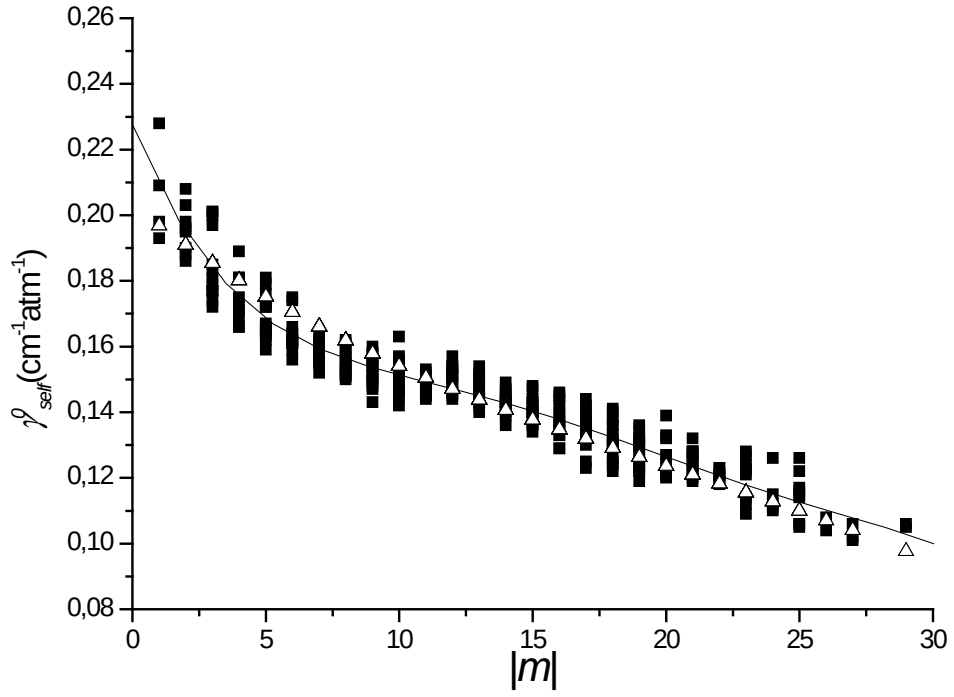

Fig. 7. Rotational dependence of the self-broadening coefficients for all measurements in the 1.7-μm region. The solid line is the polynomial fit of the whole set of these measurements and the empty circles are the self-broadening coefficients calculated with the polynomial found in the 1.9-μm region.

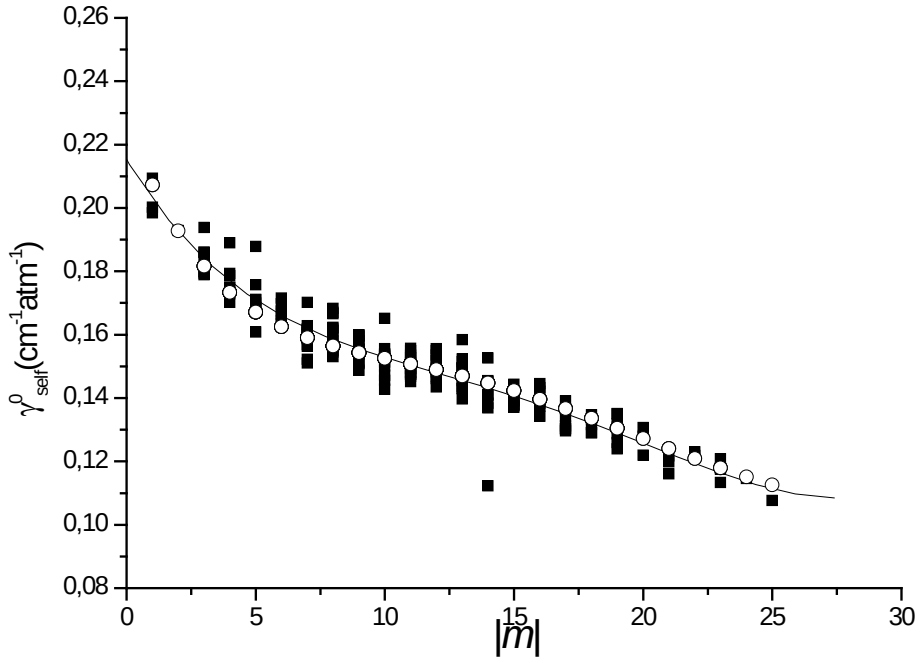

Fig. 8. Self-shifting coefficients δ^0_{self} for the $\nu_2 + \nu_3$ band.

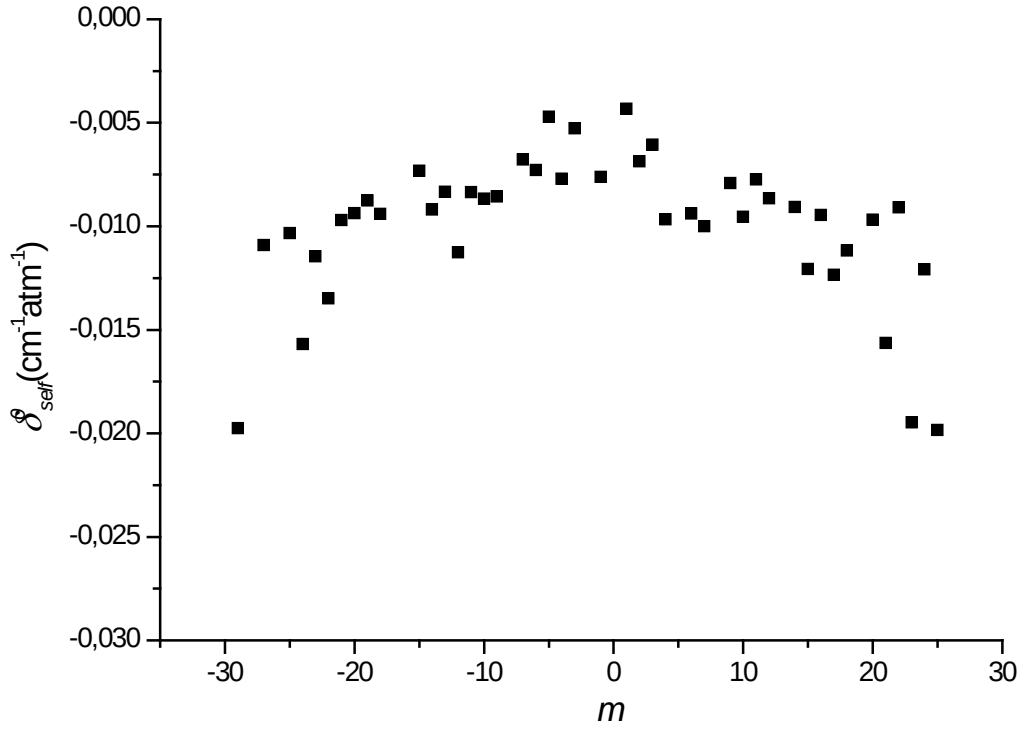

Fig. 9. Self-shifting coefficients δ^0_{self} for the $2\nu_2 + (\nu_4 + \nu_5)^0_+$ band.

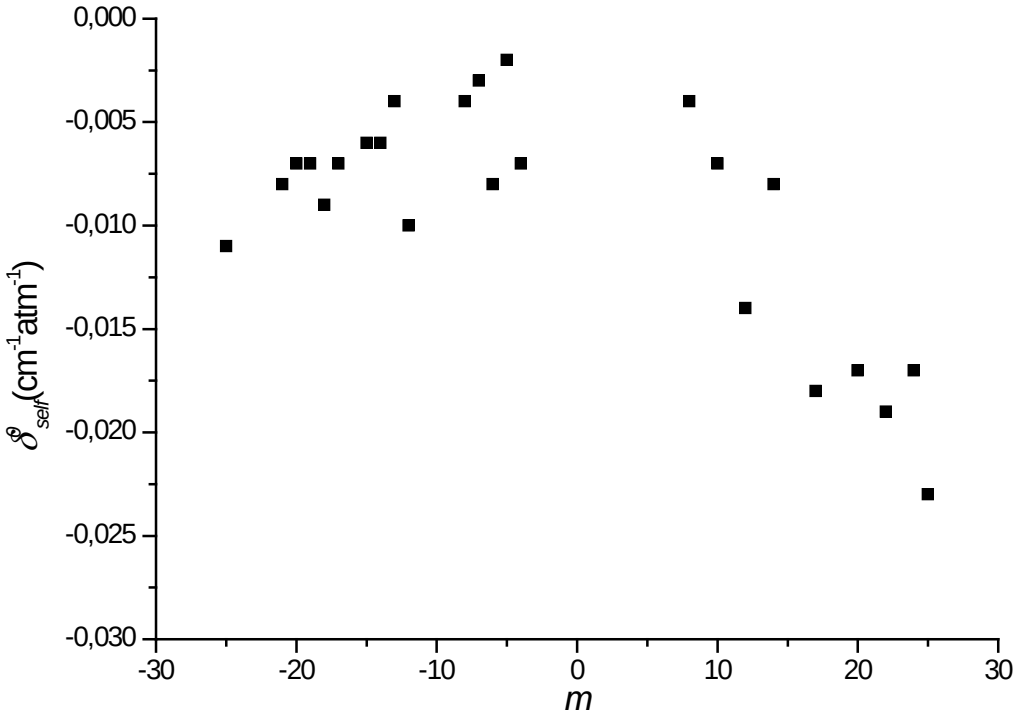

Fig. 10. The whole set of the self-shifting coefficients δ^0_{self} measured in the 1.9-μm region.

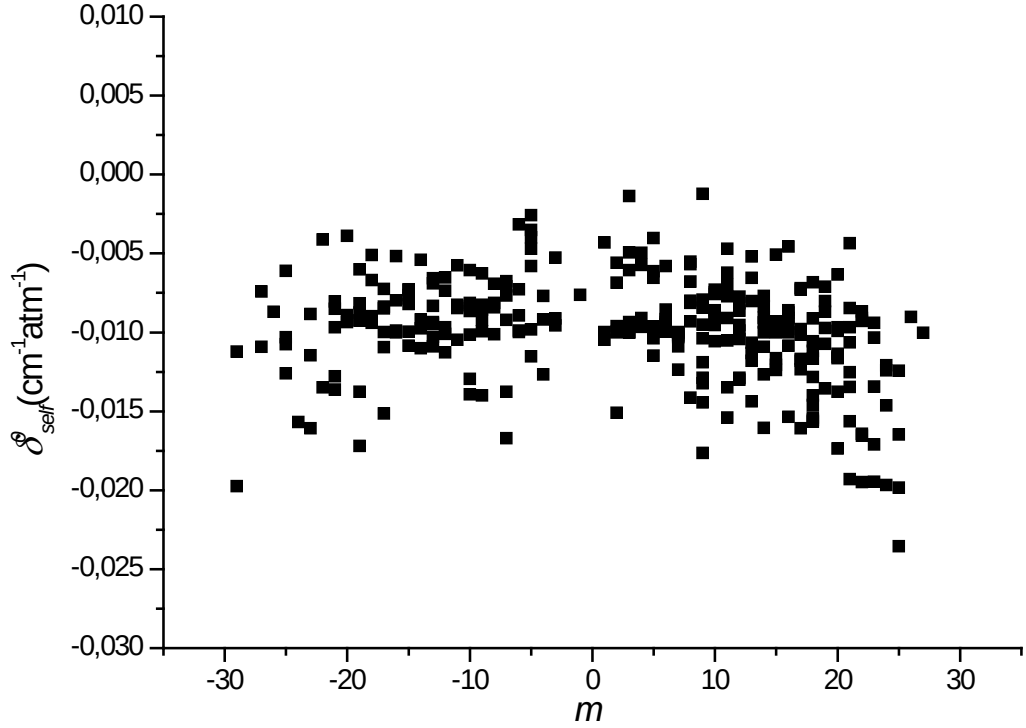

Fig. 11. Self-shifting coefficients δ^0_{self} for the $\nu_2 + \nu_3 + \nu_4{}^1$ band.

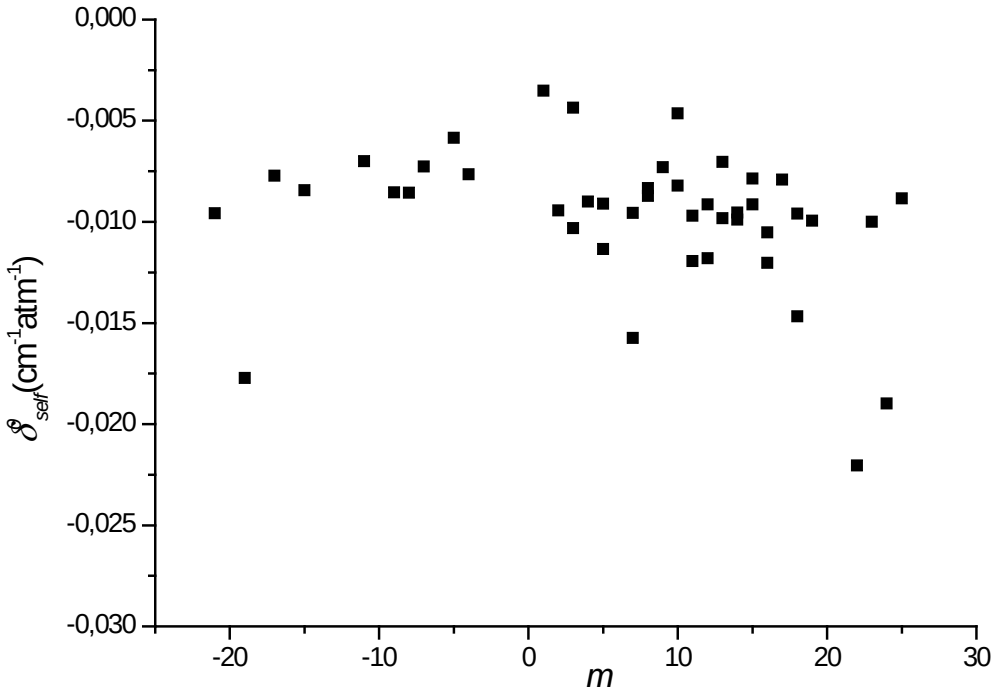

Fig. 12. The whole set of the self-shifting coefficients δ^0_{self} measured in the 1.7-μm region.